Jilin Daxue Xuebao (Gongxueban)/Journal of Jilin University (Engineering and Technology Edition)
ISSN: 1671-5497
E-Publication: Online Open Access
Vol: 42 Issue: 11-2023
DOI: 10.5281/zenodo.10153201

CONVECTION IN A HORIZONTAL LAYER OF MAXWELL NANOFLUID WITH NO FLUX OF NANOPARTICLES AT THE BOUNDARIES

JAIMALA BISHNOI
Department of Mathematics, Ch. Charan Singh University, Meerut, 250004, UP, India.
Email : jaimalaccsu@gmail.com, ORCID ID: 0000-0001-5191-5081

ARUN KUMAR*
Department of Mathematics, Ch. Charan Singh University, Meerut, 250004, UP, India.
*Corresponding Author Email: arunkumargccsu@gmail.com, ORCID ID: 0000-0001-5915-0896

Abstract

The study investigates the onset of convection in a Maxwell nanofluid layer confined between two parallel plates. This investigation takes into account thermophoretic and Brownian diffusion and assumes no nanoparticle flux at the boundaries. The analysis involves two main approaches. Linear stability analysis, under which the Galerkin-type weighted residual technique, is employed to discuss the occurrence of both stationary and oscillatory convection for various parameters. Weakly nonlinear stability analysis, under which the truncated Fourier series is utilized. Heat and mass transfer are examined for both steady and unsteady states, with a focus on assessing Nusselt numbers for heat transfer and concentration Nusselt numbers for mass transfer. The results of the analysis are visualized through various graphical representations, including the streamline distribution, isotherm distribution, and isonano concentration distribution.

Keywords: Brownian Motion, Linear and Non-Linear Instability, Maxwell Nanofluid, No Flux of Nanoparticles at The Boundaries, Heat and Mass Transfer, Galerkin-Type Weighted Residual Approach. Thermophoresis.

1. INTRODUCTION

In 1992, Choi and his research team embarked on a mission to address the technical challenges stemming from rising heat burdens, intensified heat flows, and amplified pressure differentials within diverse sectors. They were looking for an economically viable fluid solution with the highest possible thermal conductivity, achieved with minimal volume concentrations, ideally below 1% by volume. Their initial breakthrough came in the form of liquid nitrogen within microchannel heat exchangers, which exhibited exceptional heat removal capabilities for high heat load silicon mirrors used in X-ray applications. Following extensive research efforts (as documented in references [1-3]), they introduced nanofluids characterized by superior thermal conductivity and rheological properties compared to conventional fluids. Nanofluids displayed a remarkable array of advantageous traits including a substantially increased specific surface area, leading to unexpected enhancements in thermal conductivity, reactivity, and surface wettability. Additionally, nanofluids exhibited high dispersion stability, necessitating reduced pumping power to achieve equivalent heat transfer intensity. They also exhibited diminished particle agglomeration, thereby promoting the miniaturization of components and reducing surface erosion. Intriguingly, nanofluids could exhibit unusual catalytic, magnetic, or optical behaviours. These distinctive characteristics rendered nanofluids of paramount importance for a wide spectrum of scientific and technical applications. Their

Jilin Daxue Xuebao (Gongxueban)/Journal of Jilin University (Engineering and Technology Edition)
ISSN: 1671-5497
E-Publication: Online Open Access
Vol: 42 Issue: 11-2023
DOI: 10.5281/zenodo.10153201

developments [4-7] marked a significant stride in the quest to address challenges related to heat management and transfer in various industries. These researches opened up new avenues for improving heat transfer efficiency in various industries, ranging from electronics cooling to energy systems. Nanofluids are observed as Newtonian fluids [8-9] as well as non-Newtonian fluids [10-11].

As a part of the International Nanofluid Property Benchmark Exercise (INPBE) [12], an effort was made to study the rheology of nanofluids [13]. Chen et al. [14] observed that the nanofluid's shear-thinning characteristics are contingent upon the particle volume fraction and the value of shear rates. For the volume fraction, $\phi < 0.001$, shear thinning is absent. However, when $0.001 < \phi < 0.05$, shear thinning becomes evident at low shear rates, and when ϕ exceeds 0.05, shear thinning behaviour is anticipated across the entire range of shear rates. Duan et al. [10] showed the effect of particle aggregation on the non-Newtonian behaviour of nanofluid. Chen and Ding [15] in their detailed rheological discussion of nanofluids showed that the Newtonian or non-Newtonian behaviour of nanofluids depends on particle size and shape, particle concentration, base liquid viscosity and solution chemistry. Hojjat et al. [16] studied the rheological characteristics of non-Newtonian nanofluids with experimental investigation. They observed that all types of nanofluids as well as the base fluid exhibit behaviour as pseudoplastic fluids. During the last decade, several studies of a wide range of nanofluids with a diverse composition, have found that nanofluids behave like non-Newtonian and hybrid fluids [17-26].

Maxwell [27] introduced a significant class of non-Newtonian fluids characterized by their unique energy behaviour during deformation. Unlike traditional fluids, these fluids do not retain 100% of the energy applied to them but instead dissipate a portion. This distinctive characteristic manifests as a simultaneous display of both elastic and viscous properties. Examples of such fluids encompass glycerine, toluene, crude oil, flour dough, and dilute polymeric solutions, among others. The presence of nanoparticles in Maxwell fluids changes their rheological properties making them potentially applicable in various fields, including dampers and shock absorbers in vehicles, haptic feedback devices, and adaptive optics. Umavathi et al. [28] conducted a study on the double-diffusive convection within a horizontal Maxwell nanofluid-saturated porous medium by utilizing the modified Darcy-Maxwell model. Umavathi and Mohite [29] conducted the stability analysis, both linear and weakly non-linear, to investigate the convection in a porous medium-saturated horizontal layer containing a Maxwell nanofluid. Ramzan et al. [30] explored the mixed convective flow of a Maxwell nanofluid with Soret and Dufour effects through a porous medium.They also considered the influence of variable temperature and concentration on a linearly permeable stretched surface. Jaimala et al. [31] extended the classical Horton-Rogers-Lapwood problem to the Maxwell nanofluid in the framework of Buongiorno's nanofluid model in which effects of thermophoretic and Brownian diffusions are incorporated in the flow. Jaimala et al. [32] investigated the double-diffusive convection in a Darcy Maxwell Buongiorno's nanofluid by stimulating the flow with a modified Darcy-Maxwell fluid model with the assumption of zero flux of nanoparticles at the boundaries. Sharma et al. [33] explored how the rheological properties of a Maxwell fluid impact natural convection in a dielectric nanofluid subjected to a vertical AC electric field. Singh et al. [34] investigated the movement of salt particles induced by a thermal gradient and

Jilin Daxue Xuebao (Gongxueban)/Journal of Jilin University (Engineering and Technology Edition)
ISSN: 1671-5497
E-Publication: Online Open Access
Vol: 42 Issue: 11-2023
DOI: 10.5281/zenodo.10153201

the drift of nanoparticles caused by Brownian motion within a Darcy porous medium saturated with a Maxwellian nanofluid where the flux of nanoparticles is influenced by Stefan's boundary flow conditions. Singh et al. [35] also delved into the study of triple diffusive convection with Soret-Dufour effects in a macroscopic filtration model for Darcy porous medium saturated by a Maxwellian nanofluid. Aziz and Shams [36] studied the influence of the internal heat source on the volumetric rate of entropy generation in an electrically conducting Maxwell nanofluid flowing over a penetrable stretching sheet subjected to variable thermal conductivity and thermal radiation. Xu et al. [37] explored the horizontal flow of an incompressible, steady Maxwell nanofluid containing gyrotactic microorganisms, with a focus on energy transfer. Khan et al. [38] examined the effects of heat and mass transfer on the transient incompressible flow of a Maxwell nanofluid, which was formulated using engine oil as the base fluid and molybdenum disulfide as suspended nanoparticles. This investigation was conducted over an infinite vertical plate featuring both ramped and isothermal wall temperature and concentration profiles. Wang et al. [39] considered the slip effects and convective boundary conditions and explored the inherent bio-convective motion of a Maxwell nanofluid across an exponentially stretching interface. Khan et al. [40] found the profiles for the velocity, temperature, and concentration distributions for an open channel flow of a grease-based Maxwell fluid with MoS_2 nanoparticles suspended in it. Sangeetha et al. [41] incorporated Hall and ion effects into their investigation of a Maxwell fluid carrying gyrotactic microorganisms and nanoparticles in a non-Darcy porous environment. The study emphasizes the analysis of various factors, including bioconvection phenomena, thermal radiation, heat generation/absorption effects, and chemical reactions.

Based on the literature reviewed, there appears to be a noticeable gap in research concerning the flow behaviour of Maxwell nanofluids between parallel plates. The flow of fluids between parallel plates holds significant relevance in both research and industrial contexts. Such flow configurations find applications in a wide range of areas, including, but not limited to, metal lubrication in bearings, food production processes, cooling towers, hydrodynamic devices, the petrochemical industry, fog generation and dispersion, as well as polymer processing. In highly conductive fluids or at low temperatures, like in many HVAC systems (Heating, Ventilation, and Air conditioning systems), the radiation is usually negligible compared to the heating from radiators. Further, in heat transfer applications involving nanofluids, such as in cooling systems or heat exchangers, the achievement of local thermal equilibrium ensures efficient heat transfer between the fluid and the solid nanoparticles, leading to more predictable and controllable thermal performance. Therefore, in this study, we aim to investigate the convection in a horizontal layer of Maxwell nanofluid confined between two parallel plates when there is no radiative heat transfer and fluid and the nanoparticles are in local thermal equilibrium (LTE).

It is worth noting that previous research has primarily focused on controlling and maintaining a constant mass flux of nanoparticles at the boundaries. Initially, Nield and Kuznetsov [42] analysed thermal convection in a Newtonian nanofluid within a porous medium, assuming that the nanoparticle fraction at the boundaries can be managed in a similar manner as temperature control. However, because nanoparticles are typically on

Jilin Daxue Xuebao (Gongxueban)/Journal of Jilin University (Engineering and Technology Edition)
ISSN: 1671-5497
E-Publication: Online Open Access
Vol: 42 Issue: 11-2023
DOI: 10.5281/zenodo.10153201

the nanoscale, their size is much smaller than the characteristic length scales of the bounding surfaces. Consequently, nanoparticles experience minimal gravitational settling and have limited interaction with solid surfaces. Furthermore, their concentration near boundaries is typically lower than in the bulk region, reducing the likelihood of particle accumulation at the surfaces. Stabilizing forces help maintain a homogeneous suspension, thus preventing significant nanoparticle flux to the surfaces. In our study, we consider a more realistic scenario with no nanoparticle flux at the boundaries. We employ linear stability analysis and utilize the Galerkin-type weighted residuals method to examine the impact of various pertinent parameters on both stationary and oscillatory convection. Additionally, we employ non-linear stability theory to discuss the mechanisms of heat and mass transfer. We discuss convection both analytically and numerically.

2. FORMULATION OF THE PROBLEM

Consider an infinite horizontal layer of Maxwell viscous nanofluid with a finite depth under the influence of vertically downward gravitational force. The initial state is characterized by the absence of flow and is subjected to a negative thermal gradient, which extends upward through the layer. It is considered that

- the radiative heat transfer is neglected
- viscous dissipation is negligible
- the concentration of reactive species (e.g., chemicals) within the fluid is negligible
- nanoparticles and base fluid are in local thermal equilibrium
- there is no flux of nanoparticles at the boundaries (Baehr and Stephan [43] and Nield and Kuznetsov [44]).
- boundaries are perfectly heat-conducting with $T^*_h > T^*_c$

Figure 1 refers to the illustration depicting the physical configuration of the problem under consideration

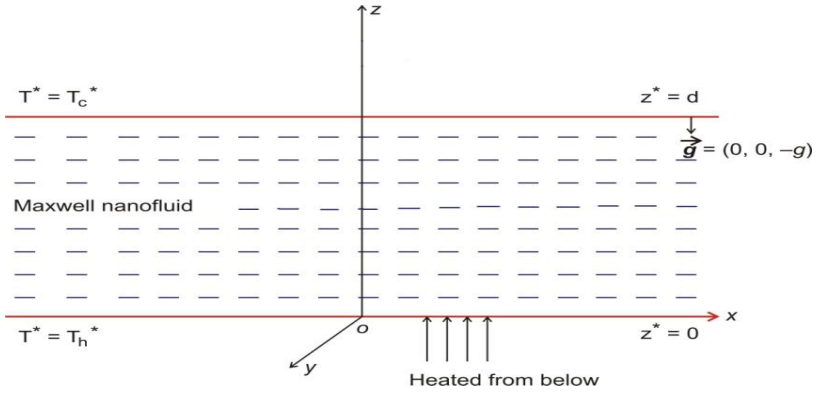

Fig 1: Physical Configuration

Jilin Daxue Xuebao (Gongxueban)/Journal of Jilin University (Engineering and Technology Edition)
ISSN: 1671-5497
E-Publication: Online Open Access
Vol: 42 Issue: 11-2023
DOI: 10.5281/zenodo.10153201

Following Buongiorno [45], Umavathi and Mohite [29] and Sharma et al. [33], the mass, momentum and energy conservation equations for a Maxwell nanofluid and boundary conditions against the passive management of nanoparticles (Nield and Kuznetsov [44]), are taken as

$$\nabla^* \cdot \mathbf{v}^* = 0, \tag{1}$$

$$\rho\left(1+\lambda^*\frac{\partial}{\partial t^*}\right)\left(\frac{\partial}{\partial t^*}+\mathbf{v}^*\cdot\nabla^*\right)\mathbf{v}^* = \left(1+\lambda^*\frac{\partial}{\partial t^*}\right)\left[-\nabla^* p^* + \left\{\phi^*\rho_p + \left(1-\phi^*\right)\left\{\rho\left(1-\beta\left(T^*-T_c^*\right)\right)\right\}\right\}\mathbf{g}\right] + \mu\nabla^{*2}\mathbf{v}^*, \tag{2}$$

$$\left(\rho c\right)_f\left[\frac{\partial}{\partial t^*}+\mathbf{v}^*\cdot\nabla^*\right]T^* = k\nabla^{*2}T^* + \left(\rho c\right)_p\left[D_B\nabla^*\phi^*\cdot\nabla^*T^* + \left(D_T/T_c^*\right)\nabla^*T^*\cdot\nabla^*T^*\right], \tag{3}$$

$$\frac{\partial\phi^*}{\partial t^*}+\mathbf{v}^*\cdot\nabla^*\phi^* = D_B\nabla^{*2}\phi^* + \left(D_T/T_c^*\right)\nabla^{*2}T^*, \tag{4}$$

$$\mathbf{v}^* = 0, \quad T^* = T_h^*, \quad D_B\frac{\partial\phi^*}{\partial z^*}+\frac{D_T}{T_c^*}\frac{\partial T^*}{\partial z^*} = 0 \quad \text{at } z^* = 0, \tag{5}$$

$$\mathbf{v}^* = 0, \quad T^* = T_c^*, \quad D_B\frac{\partial\phi^*}{\partial z^*}+\frac{D_T}{T_c^*}\frac{\partial T^*}{\partial z^*} = 0 \quad \text{at } z^* = d, \tag{6}$$

where $\mathbf{v}^*$ is the velocity vector, λ^* is the stress relaxation time, ρ is the density of fluid , p^* is the hydrostatic pressure, ϕ^* is the nanoparticle volume fraction, ρ_p is the density of nanoparticles, t^* is the time, T_c^* is the reference temperature, T_h^* is the temperature at the lower boundary , T^* is the temperature, β is the thermal expansion coefficient of the fluid, g is the gravitational acceleration vector, d is the depth between two boundaries , μ is the viscosity, $(\rho c)_f$ and $(\rho c)_p$ are the heat capacity of nanofluid and nanoparticles respectively, k is the thermal conductivity of nanofluid, D_B is the Brownian diffusion coefficient and D_T is the thermophoretic diffusion coefficient. Dimensional variables are denoted by asterisks.

Introduce the following non-dimensional variables in Eqs. (1) to (6):

$$(x,y,z) = \frac{(x^*,y^*,z^*)}{d},\ p = \frac{p^*d^2}{\mu\alpha_f},\ (u,v,w) = \frac{(u^*,v^*,w^*)d}{\alpha_f},$$

$$t = \frac{t^*\alpha_f}{d^2},\ \phi = \frac{\phi^*-\phi_0^*}{\phi_0^*},\ T = \frac{T^*-T_c^*}{T_h^*-T_c^*},\ \lambda = \frac{\lambda^*\alpha_f}{d^2} \text{ and } \alpha_f = \frac{k_f}{(\rho c)_f}, \tag{7}$$

Jilin Daxue Xuebao (Gongxueban)/Journal of Jilin University (Engineering and Technology Edition)
ISSN: 1671-5497
E-Publication: Online Open Access
Vol: 42 Issue: 11-2023
DOI: 10.5281/zenodo.10153201

and get

$$\nabla \cdot \mathbf{v} = 0\,, \tag{8}$$

$$\frac{1}{\mathrm{Pr}}\left(1+\lambda\frac{\partial}{\partial t}\right)\left(\frac{\partial \mathbf{v}}{\partial t}+\mathbf{v}\cdot\nabla\mathbf{v}\right)=\left(1+\lambda\frac{\partial}{\partial t}\right)\left(-\nabla p - Rn\phi\,\hat{\mathbf{e}}_{\mathbf{z}} - Rm\hat{\mathbf{e}}_{\mathbf{z}} + RaT\hat{\mathbf{e}}_{\mathbf{z}}\right)+\nabla^2\mathbf{v}\,, \tag{9}$$

$$\frac{\partial T}{\partial t}+\mathbf{v}.\nabla T=\nabla^2 T+\frac{N_B}{Le}\nabla\phi.\nabla T+\frac{N_A N_B}{Le}\nabla T.\nabla T\,, \tag{10}$$

$$\frac{\partial \phi}{\partial t}+\mathbf{v}.\nabla\phi=\frac{1}{Le}\nabla^2\phi+\frac{N_A}{Le}\nabla^2 T\,, \tag{11}$$

$$\mathbf{v}=0,\quad T=1,\quad \frac{\partial\phi}{\partial z}+N_A\frac{\partial T}{\partial z}=0\quad \text{at } z=0, \tag{12}$$

$$\mathbf{v}=0,\quad T=0,\quad \frac{\partial\phi}{\partial z}+N_A\frac{\partial T}{\partial z}=0\quad \text{at } z=1\,, \tag{13}$$

where $\nabla^2 \equiv \frac{\partial^2}{\partial x^2}+\frac{\partial^2}{\partial y^2}+\frac{\partial^2}{\partial z^2}$ is the three–dimensional Laplacian operator.

The non-dimensional thermo-physical parameters introduced in Eqs. (9)-(13) are $Ra=\frac{\rho g\beta d^3(T_h^*-T_c^*)}{\mu\alpha_f}$ (the thermal Rayleigh number), $Rm=\frac{\left\{\rho_p\phi_0^*+\rho(1-\phi_0^*)\right\}gd^3}{\mu\alpha_f}$ (the basic density Rayleigh number), $Rn=\frac{(\rho_p-\rho)\phi_0^* gd^3}{\mu\alpha_f}$ (the nanoparticle concentration Rayleigh number), $N_A=\frac{D_T(T_h^*-T_c^*)}{D_B T_c^*\phi_0^*}$ (the modified diffusivity ratio), $N_B=\frac{(\rho c)_p}{(\rho c)_f}\phi_0^*$ (the modified particle density ratio), $\mathrm{Pr}=\frac{\mu}{\rho\alpha_f}$ (the Prandtl number) and $Le=\frac{\alpha_f}{D_B}$ (the Lewis number).

3. BASIC STATE SOLUTION PROCEDURE

Consider the stationary state

$$\mathbf{v}=0\,,\phi=\phi_b(z)\,,p=p_b(z)\ \text{and}\ T=T_b(z). \tag{14}$$

The state given by (14) leads to the following equations:

$$\frac{dp_b}{dz}+Rn\phi_b+Rm-RaT_b=0\,, \tag{15}$$

$$\frac{d^2T_b}{dz^2}+\frac{N_B}{Le}\frac{d\phi_b}{dz}\frac{dT_b}{dz}+\frac{N_A N_B}{Le}\left(\frac{dT_b}{dz}\right)^2=0\,, \tag{16}$$

Jilin Daxue Xuebao (Gongxueban)/Journal of Jilin University (Engineering and Technology Edition)
ISSN: 1671-5497
E-Publication: Online Open Access
Vol: 42 Issue: 11-2023
DOI: 10.5281/zenodo.10153201

$$\frac{d^2\phi_b}{dz^2} + N_A \frac{d^2 T_b}{dz^2} = 0. \tag{17}$$

Eqs. (15) - (17) subjected to the boundary conditions given by Eqs. (12) and (13), provide the approximated basic solutions for the temperature and concentration as

$$T_b = 1 - z\,, \tag{18}$$

$$\phi_b = \phi_0 + N_A z. \tag{19}$$

4. PERTURBED STATE SOLUTION PROCEDURE

The basic state is subjected to infinitesimal perturbations and the concerned parameters are assumed as

$$\mathbf{v} = \mathbf{v}'\,,\ T = T_b + T'\,,\ \ \phi = \phi_b + \phi' \ \text{ and } \ p = p_b + p'\,. \tag{20}$$

On substituting the perturbed values of parameters defined in (20) into Eqs. (8) - (13), we get

$$\nabla \cdot \mathbf{v}' = 0\,, \tag{21}$$

$$\frac{1}{\mathrm{Pr}}\left(1 + \lambda \frac{\partial}{\partial t}\right)\left(\frac{\partial}{\partial t} + \mathbf{v}' \cdot \nabla\right)\mathbf{v}' = \left(1 + \lambda \frac{\partial}{\partial t}\right)\left\{-\nabla p' - Rn\phi' \hat{\mathbf{e}}_z + RaT' \hat{\mathbf{e}}_z\right\} + \nabla^2 \mathbf{v}', \tag{22}$$

$$\frac{\partial T'}{\partial t} + \left(\mathbf{v}' \cdot \nabla\right)T' - w' = \nabla^2 T' + \frac{N_B}{Le}\left(\frac{\partial T'}{\partial z} - 1\right)\frac{\partial \phi'}{\partial z} - \frac{N_A N_B}{Le}\frac{\partial T'}{\partial z} + \frac{N_A N_B}{Le}\left(\frac{\partial T'}{\partial z}\right)^2, \tag{23}$$

$$\frac{\partial \phi'}{\partial t} + \mathbf{v}' \cdot \nabla \phi' + w' N_A = \frac{1}{Le}\nabla^2 \phi' + \frac{N_A}{Le}\nabla^2 T'\,. \tag{24}$$

$$w' = 0,\ T' = 0,\ \frac{\partial \phi'}{\partial z} + N_A \frac{\partial T'}{\partial z} = 0 \ \text{ at } \ z = 0, 1\,. \tag{25}$$

Eliminating p' from Eq. (22) by using the operator $\hat{k} \cdot curlcurl$ and identity $curlcurl \equiv grad\ div - \nabla^2$ we get

$$\frac{1}{\mathrm{Pr}}\left(1 + \lambda \frac{\partial}{\partial t}\right)\left\{\frac{\partial}{\partial t}\left(\nabla^2 w'\right) + \nabla^2\left(w' \nabla w'\right)\right\} = \left(1 + \lambda \frac{\partial}{\partial t}\right)\left\{Ra \nabla_H{}^2 T' - Rn \nabla_H{}^2 \phi'\right\} + \nabla^4 w'\,, \tag{26}$$

where $\nabla_H{}^2 = \dfrac{\partial^2}{\partial x^2} + \dfrac{\partial^2}{\partial y^2}$ is the two-dimensional Laplacian operator in the x-y plane.

Jilin Daxue Xuebao (Gongxueban)/Journal of Jilin University (Engineering and Technology Edition)
ISSN: 1671-5497
E-Publication: Online Open Access
Vol: 42 Issue: 11-2023
DOI: 10.5281/zenodo.10153201

5. INVESTIGATION UNDER LINEAR STABILITY THEORY

Allowing the perturbations to be of the form

$$(w', T', \phi') = [W(z), \theta(z), \Phi(z)] \exp(ilx + imy + st), \tag{27}$$

where l and m are the wave number in x and y directions respectively and s is the growth rate of perturbations, Eqs. (23) to (26) become and reordered as

$$(1+\lambda s)\left(\frac{s}{\mathrm{Pr}}\left(D^2-\alpha^2\right)W + \alpha^2 Ra\theta - \alpha^2 Rn\Phi\right) - \left(D^2-\alpha^2\right)^2 W = 0, \tag{28}$$

$$W + \left(D^2 - \frac{N_A N_B}{Le} D - \alpha^2 - s\right)\theta - \frac{N_B}{Le} D\Phi = 0, \tag{29}$$

$$N_A W - \frac{N_A}{Le}\left(D^2-\alpha^2\right)\theta - \left(\frac{1}{Le}(D^2-\alpha^2) - s\right)\Phi = 0, \tag{30}$$

$$W = 0, \quad \theta = 0, \quad D\Phi + N_A D\theta = 0 \quad \text{at } z = 0 \text{ and } z = 1, \tag{31}$$

where $\alpha^2 = l^2 + m^2$ and $D \equiv \frac{d}{dz}$.

In the context of the Galerkin-type weighted residual method for approximating solutions to Eqs. (28) - (31), we opt for the following trial functions satisfying the boundary conditions (31):

$$W = \sum_{p=1}^{N} A_p \sin p\pi z, \ \theta = \sum_{p=1}^{N} B_p \sin p\pi z, \ \Phi = -\sum_{p=1}^{N} C_p N_A \sin p\pi z \ \text{with} \ \ p = 1, 2, 3, \ldots .. N, \tag{32}$$

where A_p, B_p and C_p are constants to be determined.

Considering the first approximation and taking $N = 1$ in (32), for the existence of a non-trivial solution of Eqs. (28) - (30), the determinant of the coefficient matrix will vanish, i.e.

$$\begin{vmatrix} \left(-(1+\lambda s)\frac{s}{\mathrm{Pr}}\delta^2 - \delta^4\right) & \alpha^2(1+\lambda s)Ra & \alpha^2 N_A(1+\lambda s)Rn \\ 1 & -(\delta^2+s) & 0 \\ N_A & \frac{N_A}{Le}\delta^2 & -\left(\frac{\delta^2}{Le}+s\right)N_A \end{vmatrix} = 0, \tag{33}$$

where $\delta^2 = \pi^2 + \alpha^2$.

Eq. (33) provides the following thermal Rayleigh number:

$$Ra = \frac{\delta^2}{\alpha^2}\left\{\frac{s}{Pr} + \frac{\delta^2}{(1+\lambda s)}\right\}\left(\delta^2 + s\right) - N_A\left\{1 + \frac{\delta^2 Le}{\left(\delta^2 + sLe\right)}\right\}Rn. \tag{34}$$

Jilin Daxue Xuebao (Gongxueban)/Journal of Jilin University (Engineering and Technology Edition)
ISSN: 1671-5497
E-Publication: Online Open Access
Vol: 42 Issue: 11-2023
DOI: 10.5281/zenodo.10153201

5.1. Stationary convection

From Eq. (34), we get the stationary thermal Rayleigh number at the marginal state as:

$$Ra^{st} = \frac{\delta^6}{\alpha^2} - N_A\left(1+Le\right)Rn\,. \tag{35}$$

From Eq. (35) the critical stationary thermal Rayleigh number Ra^{st} at the critical wave number $\alpha = \pi/\sqrt{2}$ is obtained as

$$Ra_c^{\,st} = \frac{27}{4}\pi^4 - N_A\left(1+Le\right)Rn\,. \tag{36}$$

It should be noted that though both the Darcy Maxwell nanofluid [31] and the Maxwell fluid in a continuous medium share the absence of the Maxwell relaxation parameter in their thermal Rayleigh numbers, they are distinct due to the differing non-dimensional parameters involved in each. Further, the presence of nanoparticles reduces the Rayleigh number by a substantial amount indicating that as nanoparticles are responsible for enhancing the convection in a porous medium, the convection is promoted by them in a continuous medium as well. Additionally, nanoparticles significantly lowering the Rayleigh number. This suggests that nanoparticles not only enhance convection in a porous medium [31] but also promote convection in a continuous medium. It is evident that higher values of Rn predict critical destabilization, which can be counteracted by cooling the bottom layer in relation to the top layer. This situation aligns with physical realism, as nanofluids are renowned for their higher thermal conductivity.

5.2. Oscillatory convection

For analysing the oscillatory convection, substituting $s = i\omega_i$ in Eq. (34), and dropping *i* from the suffix for convenience, the Rayleigh number for the oscillatory convection is obtained as

$$Ra^{osc} = \frac{\delta^2}{\alpha^2}\left\{\frac{\delta^4}{\left(1+\lambda^2\omega^2\right)} - \frac{\omega^2}{\mathrm{Pr}} + \frac{\omega^2\delta^2\lambda}{\left(1+\lambda^2\omega^2\right)}\right\} - N_A\left\{1+\frac{\delta^4 Le}{\left(\delta^4+\omega^2 Le^2\right)}\right\}Rn\,. \tag{37}$$

where, the frequency of oscillation ω is obtained as

$$\omega^2 = \frac{-\xi_2 + \sqrt{\xi_2^{\,2} - 4\xi_1\xi_3}}{2\xi_1}, \tag{38}$$

where $\xi_1 = \delta^2\lambda^2 Le^2$, (39)

$$\xi_2 = \delta^2\left(Le^2 + \delta^4\lambda^2 - \delta^2\lambda\,\mathrm{Pr}\,Le^2 + \mathrm{Pr}\,Le^2\right) + \alpha^2 Le^2 N_A Rn\,\mathrm{Pr}\,\lambda^2, \tag{40}$$

and $\xi_3 = \delta^6\left(1+\mathrm{Pr}\right) - \delta^8\lambda\,\mathrm{Pr} + \alpha^2 N_A\,\mathrm{Pr}\,Le^2 Rn.$ (41)

Jilin Daxue Xuebao (Gongxueban)/Journal of Jilin University (Engineering and Technology Edition)
ISSN: 1671-5497
E-Publication: Online Open Access
Vol: 42 Issue: 11-2023
DOI: 10.5281/zenodo.10153201

Here, it is clear that in view of (38), ξ_3 has to be necessarily positive, providing the condition for the existence of the oscillatory convection. Thus, the oscillatory convection which was non-existent [44,46,47,49-60] exists here though with certain restriction.

6. INVESTIGATION UNDER NON-LINEAR STABILITY THEORY

To find the mode of heat and mass transfer, the thermal Nusselt number and the concentration Nusselt number are calculated by maintaining the non-linearity of the governing equations of the flow. For two-dimensional rolls consider velocity components in terms of the stream function ψ and find the perturbed state equations of motion free from the pressure *p* and the boundary conditions as:

$$\left(1+\lambda\frac{\partial}{\partial t}\right)\left[\frac{1}{\mathrm{Pr}}\left\{\frac{\partial}{\partial t}\nabla_1^{\,2}\psi-\frac{\partial\left(\psi,\nabla_1^{\,2}\psi\right)}{\partial\left(x,z\right)}\right\}\right]=\left(1+\lambda\frac{\partial}{\partial t}\right)\left[Rn\frac{\partial\phi}{\partial x}-Ra\frac{\partial T}{\partial x}\right]+\nabla_1^{\,4}\psi, \tag{42}$$

$$\frac{\partial T}{\partial t}+\frac{\partial\psi}{\partial x}=\nabla_1^{\,2}T+\frac{\partial(\psi,T)}{\partial(x,z)}, \tag{43}$$

$$\frac{\partial\phi}{\partial t}-N_A\frac{\partial\psi}{\partial x}=\frac{1}{Le}\nabla_1^{\,2}\phi+\frac{N_A}{Le}\nabla_1^{\,2}T+\frac{\partial(\psi,\phi)}{\partial(x,z)}, \tag{44}$$

$$\psi=\frac{\partial^2\psi}{\partial z^2}=T=0,\ \frac{\partial\phi}{\partial z}+N_A\frac{\partial T}{\partial z}=0\ \text{ at } z=0,1. \tag{45}$$

where $\nabla_1^{\,2}=\frac{\partial^2}{\partial x^2}+\frac{\partial^2}{\partial z^2}$ and the dashes (“ ' ”) have been dropped for convenience.

To perform the local non-linear stability analysis, we consider the following minimal mode Fourier expressions:

$$\psi=A_{11}(t)\sin(\alpha x)\sin(\pi z), \tag{46}$$

$$T=B_{11}(t)\cos(\alpha x)\sin(\pi z)+B_{02}(t)\sin(2\pi z), \tag{47}$$

$$\phi=-N_A\left\{C_{11}(t)\cos(\alpha x)\sin(\pi z)+C_{02}(t)\sin(2\pi z)\right\}, \tag{48}$$

where $A_{11}(t)$, $B_{11}(t)$, $B_{02}(t)$, $C_{11}(t)$ and $C_{02}(t)$ the amplitudes depending upon time are to be determined.

Substituting the solutions given by Eqs. (46) - (48) into Eqs. (42) - (44) and considering the orthogonality condition with the eigenfunctions, we obtain

$$\frac{d^2A_{11}}{dt^2}=-\frac{\mathrm{Pr}}{\lambda\delta^2}\left(\delta^4A_{11}+\alpha RnN_AC_{11}+\alpha RaB_{11}\right)-\frac{\alpha\,\mathrm{Pr}}{\delta^2}\left(RnN_A\frac{dC_{11}}{dt}+Ra\frac{dB_{11}}{dt}\right)-\frac{1}{\lambda}\frac{dA_{11}}{dt}, \tag{49}$$

$$\frac{dB_{11}}{dt}=-\left(\alpha A_{11}+\delta^2B_{11}+\alpha\pi A_{11}B_{02}\right), \tag{50}$$

Jilin Daxue Xuebao (Gongxueban)/Journal of Jilin University (Engineering and Technology Edition)
ISSN: 1671-5497
E-Publication: Online Open Access
Vol: 42 Issue: 11-2023
DOI: 10.5281/zenodo.10153201

$$\frac{dB_{02}}{dt}=\frac{1}{2}\left(\alpha\pi A_{11}B_{11}-8\pi^2 B_{02}\right), \tag{51}$$

$$\frac{dC_{11}}{dt}=-\left\{\alpha A_{11}+\alpha\pi A_{11}C_{02}-\frac{\delta^2}{Le}\left(B_{11}-C_{11}\right)\right\}, \tag{52}$$

$$\frac{dC_{02}}{dt}=\frac{1}{2}\left\{\alpha\pi A_{11}C_{11}-\frac{8\pi^2}{Le}\left(C_{02}-B_{02}\right)\right\}. \tag{53}$$

The system of simultaneous ordinary differential equations described above can be effectively addressed through numerical solutions employing the Runge-Kutta-Gill method.

In steady state, solving Eqs. (49) to (53) yield the following:

$$\frac{A_{11}^2}{8}=\frac{-\zeta_2\pm\sqrt{\zeta_2^2-4\zeta_1\zeta_3}}{2\zeta_1}, \tag{54}$$

$$B_{11}=-\frac{\alpha A_{11}}{\delta^2+\alpha^2\left(A_{11}^2/8\right)}, \tag{55}$$

$$B_{02}=-\frac{\alpha^2\left(A_{11}^2/8\right)}{\pi\left\{\delta^2+\alpha^2\left(A_{11}^2/8\right)\right\}}, \tag{56}$$

$$C_{11}=\frac{\alpha A_{11}Le}{\left\{\delta^2+\alpha^2Le^2\left(A_{11}^2/8\right)\right\}}\left\{\frac{\alpha^2\left(A_{11}^2/8\right)}{\left\{\delta^2+\alpha^2\left(A_{11}^2/8\right)\right\}}-1-\frac{\delta^2}{Le\left\{\delta^2+\alpha^2\left(A_{11}^2/8\right)\right\}}\right\}, \tag{57}$$

$$C_{02}=\frac{\alpha^2Le^2\left(A_{11}^2/8\right)}{\pi\left\{\delta^2+\alpha^2Le^2\left(A_{11}^2/8\right)\right\}}\left\{\frac{\alpha^2\left(A_{11}^2/8\right)}{\left\{\delta^2+\alpha^2\left(A_{11}^2/8\right)\right\}}-1-\frac{\delta^2}{Le\left\{\delta^2+\alpha^2\left(A_{11}^2/8\right)\right\}}\right\}$$
$$-\frac{\alpha^2\left(A_{11}^2/8\right)}{\pi\left\{\delta^2+\alpha^2\left(A_{11}^2/8\right)\right\}}, \tag{58}$$

where $\zeta_1=\alpha^2\delta^4Le^2$, (59)

$$\zeta_2=\delta^6\left(1+Le^2\right)-\alpha^2RaLe^2, \tag{60}$$

$$\zeta_3=\delta^8-\alpha^2\delta^2RnN_A\left(1+Le\right)-\alpha^2\delta^2Ra. \tag{61}$$

Jilin Daxue Xuebao (Gongxueban)/Journal of Jilin University (Engineering and Technology Edition)
ISSN: 1671-5497
E-Publication: Online Open Access
Vol: 42 Issue: 11-2023
DOI: 10.5281/zenodo.10153201

7. HEAT AND NANOPARTICLE CONCENTRATION TRANSPORT

We define the thermal Nusselt number as

$$Nu(t) = \frac{\text{Heat transfer by [conduction + convection]}}{\text{Heat transfer by conduction}}$$

$$= 1 + \left[\frac{\int_0^{2\pi/\alpha_c} \left(\frac{\partial T}{\partial z} \right) dx}{\int_0^{2\pi/\alpha_c} \left(\frac{\partial T_b}{\partial z} \right) dx} \right]_{z=0}. \tag{62}$$

Using Eqs. (18) and (47) in Eq. (62), we get

$$Nu(t) = 1 - 2\pi B_{02}(t), \tag{63}$$

by putting the value of $B_{02}(t)$ from Eq.(56) in Eq. (63), we get

$$Nu(t) = 1 + \frac{2\alpha^2 \left(A_{11}^2/8 \right)}{\left(\delta^2 + \alpha^2 \left(A_{11}^2/8 \right) \right)}. \tag{64}$$

Similarly, the nanoparticle concentration Nusselt number defined as

$$Nu_\phi(t) = 1 + \left[\frac{\int_0^{2\pi/\alpha_c} \left(\frac{\partial \phi}{\partial z} + N_A \frac{\partial T}{\partial z} \right) dx}{\int_0^{2\pi/\alpha_c} \left(\frac{\partial \phi_b}{\partial z} \right) dx} \right]_{z=0}, \tag{65}$$

is obtained with the help of Eqs. (19), (47) and (48) as

$$Nu_\phi(t) = 1 + 2\pi \left(B_{02}(t) - C_{02}(t) \right). \tag{66}$$

Use of Eqs. (56) and (58) in Eq. (66) finally provides

$$Nu_\phi(t) = 1 - \frac{2\alpha^2 Le^2 \left(A_{11}^2/8 \right)}{\left\{ \delta^2 + \alpha^2 Le^2 \left(A_{11}^2/8 \right) \right\}} \left[\frac{\alpha^2 \left(A_{11}^2/8 \right)}{\left\{ \delta^2 + \alpha^2 \left(A_{11}^2/8 \right) \right\}} - 1 - \frac{\delta^2}{Le \left\{ \delta^2 + \alpha^2 \left(A_{11}^2/8 \right) \right\}} \right]. \tag{67}$$

8. RESULTS AND DISCUSSION

8.1. Linear Stability Analysis

Figs. 2(a-c) show the behaviour of Rayleigh number Ra with respect to wave number α, in the context of the stationary convection. The behaviour of various parameters is shown by keeping the Lewis number Le, the concentration Rayleigh number *Rn*, and the modified diffusivity ratio N_A at fixed values [$Le = 100$, $Rn = 1$ and $N_A = 1$], by varying only that parameter whose behaviour is to be evaluated. It is observed that on increasing the

Jilin Daxue Xuebao (Gongxueban)/Journal of Jilin University (Engineering and Technology Edition)
ISSN: 1671-5497
E-Publication: Online Open Access
Vol: 42 Issue: 11-2023
DOI: 10.5281/zenodo.10153201

value of either the modified diffusivity ratio N_A [Fig. 2(a)], or the concentration Rayleigh number Rn [Fig. 2(b)], or the Lewis number Le [Fig. 2(c)], the critical Rayleigh number is decreased highlighting the destabilizing influence of these parameters. Since the Brownian diffusion coefficient, D_B, exhibits an inverse relationship with the Lewis number, Le the Brownian motion of nanoparticles plays a crucial role in augmenting the convection. It is worth noting that the impact of the Lewis number Le in this context is contrary to its effect on the Newtonian nanofluid or Maxwell nanofluid saturated in a porous medium [29,48] and in agreement with the convection in a Rivlin Erickson nanofluid [46]

(a)

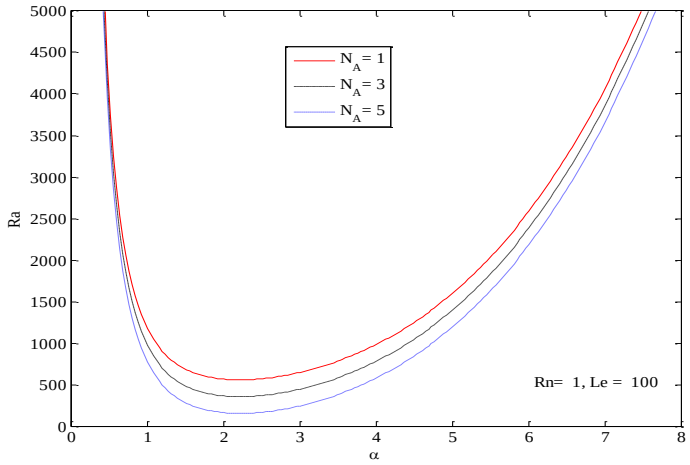

(b)

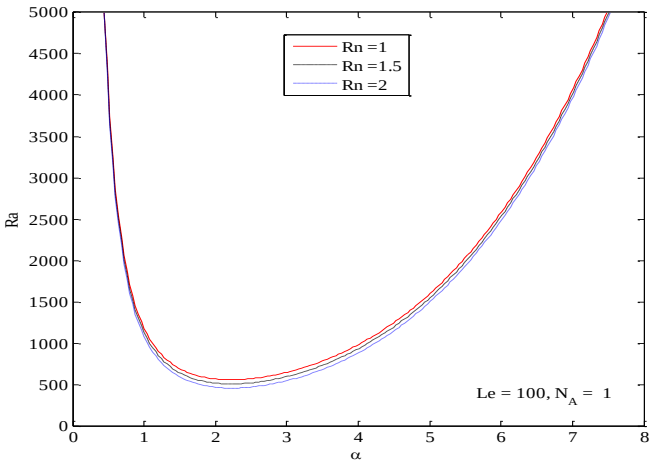

Jilin Daxue Xuebao (Gongxueban)/Journal of Jilin University (Engineering and Technology Edition)
ISSN: 1671-5497
E-Publication: Online Open Access
Vol: 42 Issue: 11-2023
DOI: 10.5281/zenodo.10153201

(c)

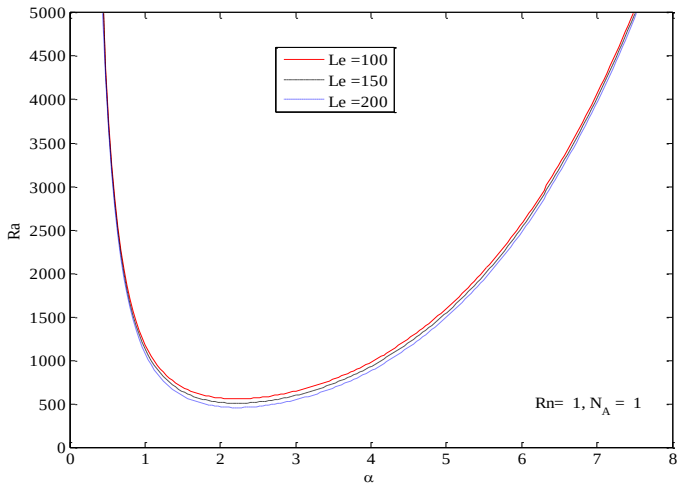

Fig 2: Trend of the stationary convection for (a) N_A, (b) Rn and (c) Le

Figs. 3(a-e) show the behaviour of the Rayleigh number Ra for oscillatory convection concerning the Lewis number Le, the Prandtl number Pr, the concentration Rayleigh number Rn, the modified diffusivity ratio N_A, and the stress relaxation parameter λ respectively. Fig. 3(a) shows that on increasing the Lewis number Le the Rayleigh number is increased which is again reverse to its effect on the oscillatory convection of a Maxwell nanofluid in a porous medium or a Maxwell nanofluid based on a macroscopic filtration model [29,31]. The effect of the Prandtl number Pr is revealed in Fig. 3(b) by fixing the other parameters. The effect of Pr is also stabilizing. Figures 3(c) to (e) explain that on increasing the values of any of the parameters, the concentration Rayleigh number Rn, the modified diffusivity ratio N_A and the stress relaxation parameter λ, the Rayleigh number is decreased i.e. all these parameters are enhancing the convection and therefore, the system is destabilized.

(a)

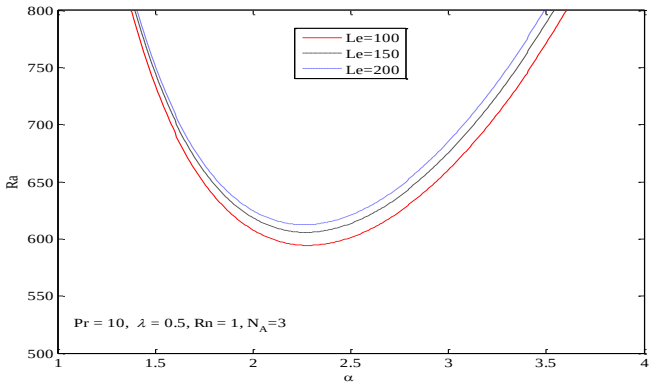

Jilin Daxue Xuebao (Gongxueban)/Journal of Jilin University (Engineering and Technology Edition)
ISSN: 1671-5497
E-Publication: Online Open Access
Vol: 42 Issue: 11-2023
DOI: 10.5281/zenodo.10153201

(b)

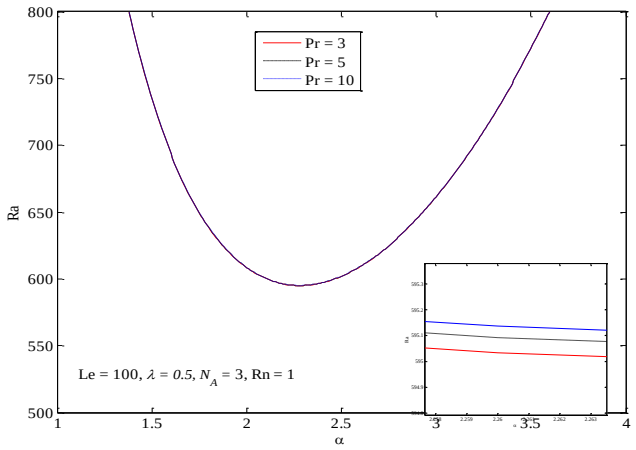

(c)

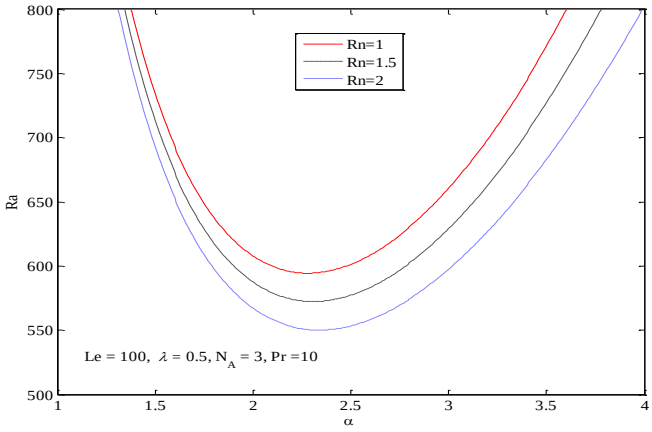

(d)

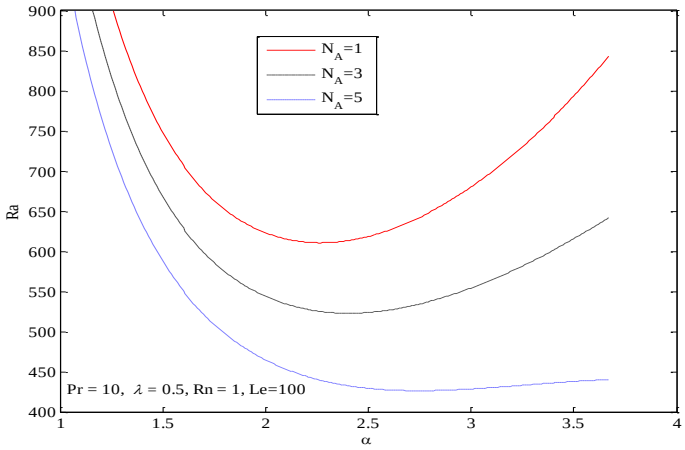

Jilin Daxue Xuebao (Gongxueban)/Journal of Jilin University (Engineering and Technology Edition)
ISSN: 1671-5497
E-Publication: Online Open Access
Vol: 42 Issue: 11-2023
DOI: 10.5281/zenodo.10153201

(e)

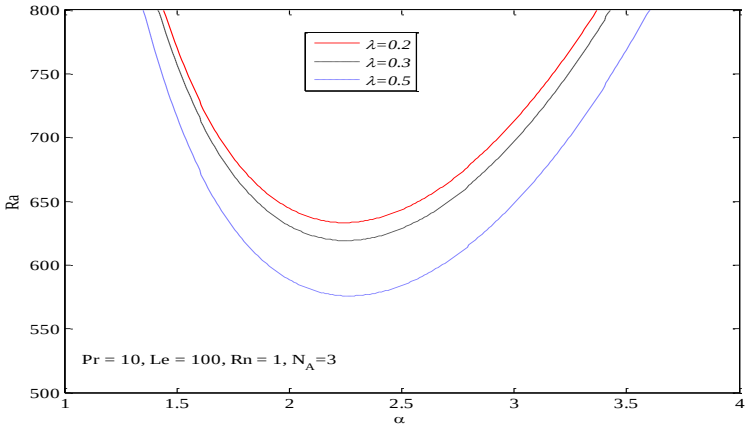

Fig 3: Trend of the oscillatory convection for (a) Le, (b) Pr, (c) Rn, (d) N_A, and (e) λ

A clear consequence for stationary as well as oscillatory convection is presented in Figs. 4(a-c). It is interesting to note that the oscillatory convection not only occurs at a later stage but it also diminishes within the wave number range of 3.8 to 5.24 for different parametric situations and finally, only stationary convection persists in all the cases.

(a)

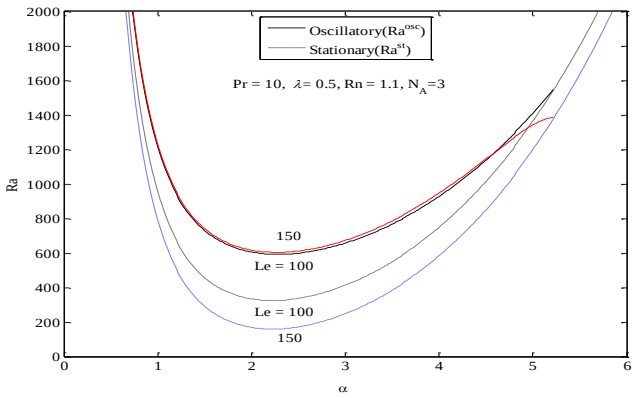

Jilin Daxue Xuebao (Gongxueban)/Journal of Jilin University (Engineering and Technology Edition)
ISSN: 1671-5497
E-Publication: Online Open Access
Vol: 42 Issue: 11-2023
DOI: 10.5281/zenodo.10153201

(b)

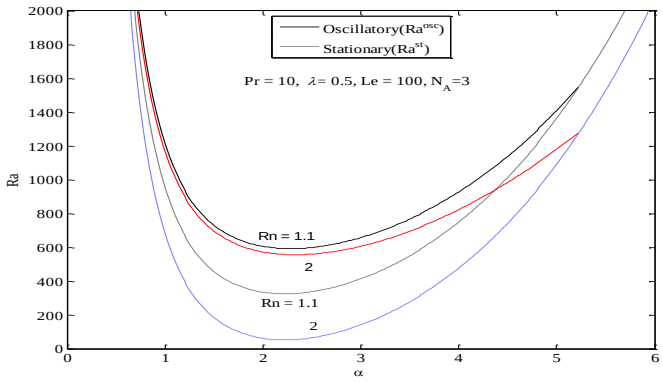

(c)

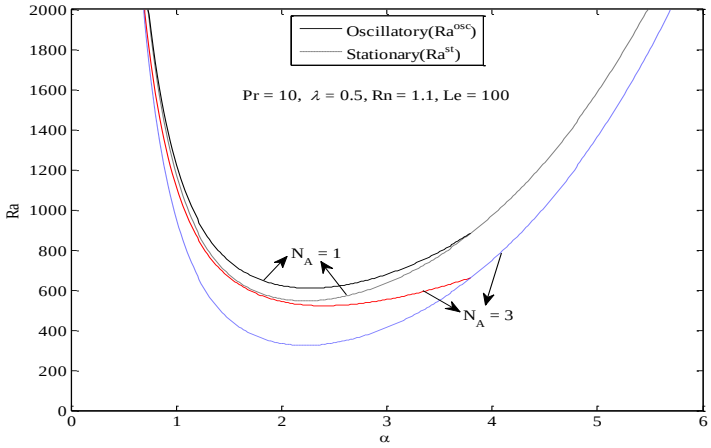

Fig4: Comparison between stationary and oscillatory convection for (a) Le, (b) Rn ,and (c) N_A

8.2. NON-LINEAR STABILITY ANALYSIS

8.2.1. Steady Analysis

For steady state (t = 0), Figs. 5(a-c) show the behaviour of the thermal Nusselt number Nu and the concentration Nusselt number Nu_ϕ with respect to the thermal Rayleigh number Ra for different values of the modified diffusivity ratio N_A, the Lewis number Le and the concentration Rayleigh number Rn. In all the figures, a common trend emerges initially, where both the heat and mass transfer rates experience a sharp increase. Additionally, it is evident that the rate of mass transfer initially surpasses that of heat transfer. However, as the thermal Rayleigh number increases, a pronounced and continuous decline in the mass transfer rate becomes apparent while the heat continues

Jilin Daxue Xuebao (Gongxueban)/Journal of Jilin University (Engineering and Technology Edition)
ISSN: 1671-5497
E-Publication: Online Open Access
Vol: 42 Issue: 11-2023
DOI: 10.5281/zenodo.10153201

to rise at a moderate rate resulting in a higher rate of transfer at and beyond a certain threshold value $(Ra^* = 1374)$.

In Figure 5(a), we examine the behaviour of the modified diffusivity ratio N_A while keeping Le and Rn fixed ($Le = 10,\ Rn = 0.1$). It is unveiled that on increasing N_A, rate of transfer of heat increases while N_A has a dual character when it comes to the rate of transfer of mass, This finding is somewhat consistent with the observations made by Jaimala et al. [31], but it differs from the convection discussed by Umavathi and Mohite [29], where an increase in N_A led to a an increase in mass transfer.

Fig. 5(b) is drawn for Rn by fixing $Le = 10$ and $N_A = 3$. It is revealed that on increasing Rn convection starts at a lower Rayleigh number Ra. It is also noticed that on increasing Rn the rate of mass transfer increases up to a certain value of Ra but after that it starts decreasing. Thus, in the steady state the dual behaviour of Rn is noticed. Here, it is worth mentioning that the behaviour of N_A and Rn concerning heat and mass transfer aligns with the observations made by Jaimala et al. [31]. However, this is in contrast to the findings of Umavathi and Mohite [29] for a Maxwell nanofluid saturated in a porous medium. In Figure 5(c), for fixed $N_A = 3$ and $Rn = 0.1$, we examine the impact of the Lewis number Le.It is evident that as Le increases, the Nusselt number Nu decreases, indicating a reduction in the heat transfer rate. Furthermore, at higher values of Le, the mass transfer parameter Nu_ϕ experiences a rapid initial increase, followed by a continuous decline. As the Rayleigh number Ra surpasses the value of 2000, this effect becomes progressively weaker, ultimately reaching a rate lower than that observed at lower Le. It's worth noting that the behaviour of Le concerning mass transfer holds true for both the flow of a Maxwell nanofluid between parallel plates, as considered here, and when it is saturated in a porous medium up to a certain Rayleigh number threshold [29,31].

(a)

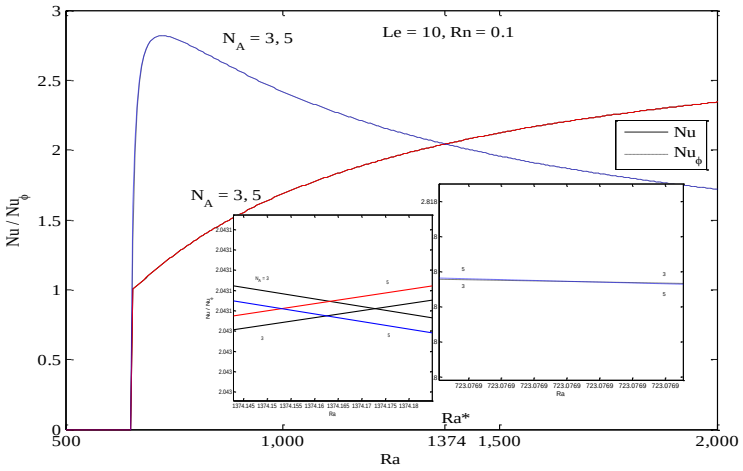

Jilin Daxue Xuebao (Gongxueban)/Journal of Jilin University (Engineering and Technology Edition)
ISSN: 1671-5497
E-Publication: Online Open Access
Vol: 42 Issue: 11-2023
DOI: 10.5281/zenodo.10153201

(b)

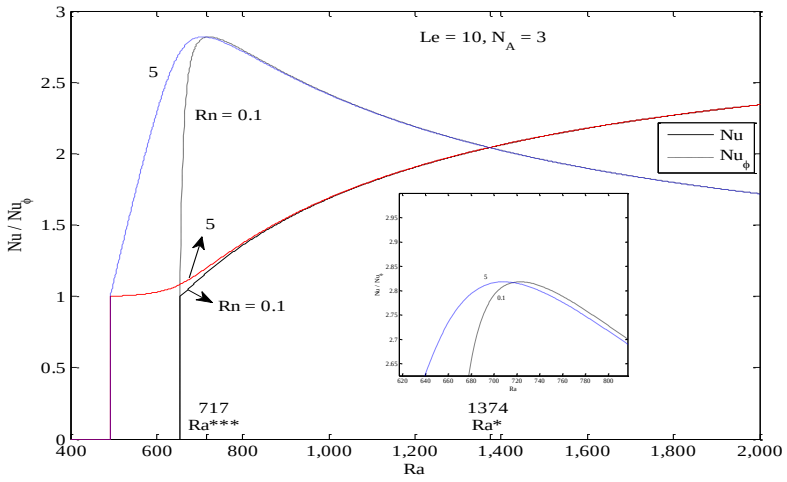

(c)

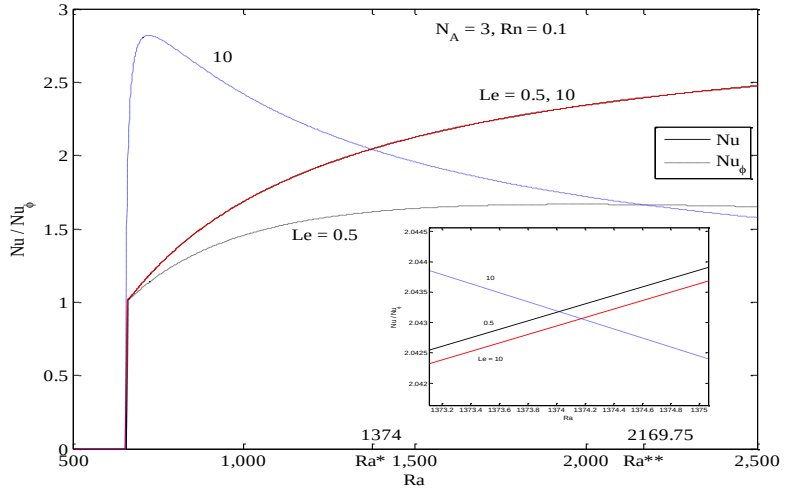

Fig 5: Steady state behaviour of Nu and Nu_ϕ vs. Ra for different values of (a) N_A, (b) Rn and (c) Le

In Fig. 6, we draw time independent flow patterns in (x-z) plane for critical thermal Rayleigh number $Ra^{cr} = 27\pi^4/4$ and $Ra = 10 \times Ra^{cr}$. The figures have been drawn for $Le = 10$, $Rn = 0.1$ and $N_A = 3$. Figs. 6(a) and 6(b) picturizing the patterns of streamlines show that the magnitude of stream function increases on increasing the value of Rayleigh number. In case of isotherms shown by figs. 6(c) and 6(d), it is clear that for critical Rayleigh number, heat transfer occurs in the form of convection but as it exceeds its critical value the convection pattern falls weak. In case of isonanoconcentrations shown

Jilin Daxue Xuebao (Gongxueban)/Journal of Jilin University (Engineering and Technology Edition)
ISSN: 1671-5497
E-Publication: Online Open Access
Vol: 42 Issue: 11-2023
DOI: 10.5281/zenodo.10153201

by figs. 6(e) and 6(f), it is clear that the mass transfer which was taking place through convection diffuses rapidly for larger Rayleigh number.

$Ra^{cr} = 27\pi^4/4$ $Ra = 10 \times Ra^{cr}$

(a) **(b)**

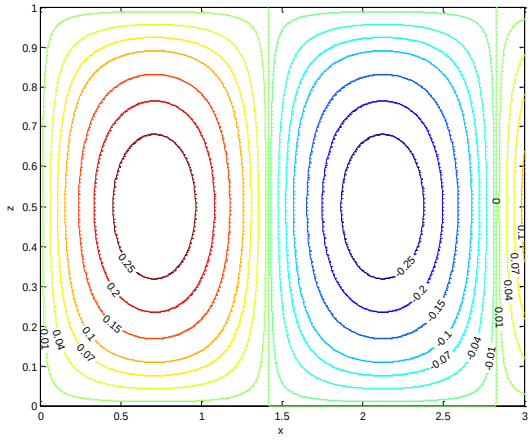

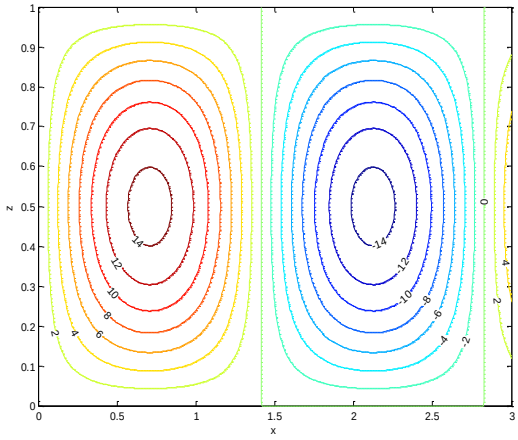

(c) **(d)**

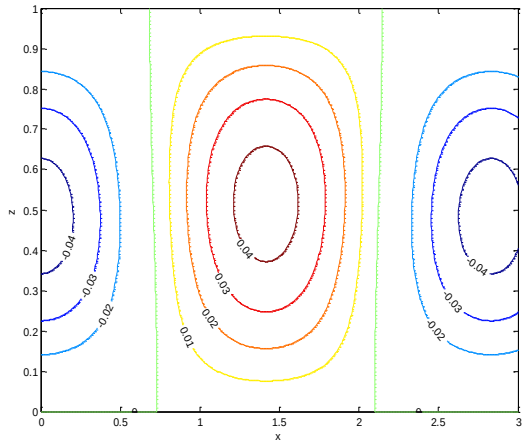

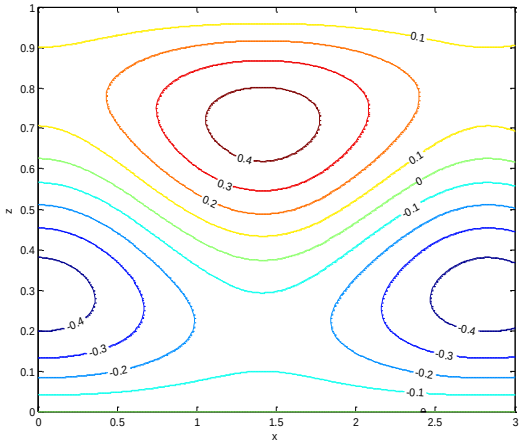

Jilin Daxue Xuebao (Gongxueban)/Journal of Jilin University (Engineering and Technology Edition)
ISSN: 1671-5497
E-Publication: Online Open Access
Vol: 42 Issue: 11-2023
DOI: 10.5281/zenodo.10153201

(e) **(f)**

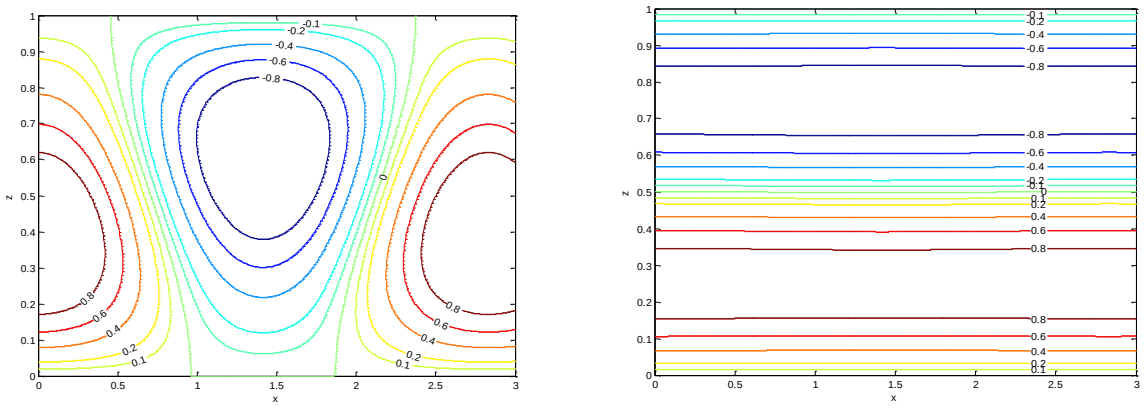

Fig.6: Time independent patterns of streamlines, isotherms and isonanoconcentrations against the thermal Rayleigh number for $Le=10$, $Rn=0.1$ and $N_A=3$

8.2.2 Unsteady Analysis

The nature of the thermal Nusselt number Nu for fluid phase and concentration Nusselt number Nu_ϕ for particle phase for unsteady state at fixed values of $Le=10$, $Rn=0.1$, $\lambda=0.5$, $\Pr=0.01$ and $N_A=3$ with variation in one of the parameters have been depicted graphically in Figs. 7(a-e) and 8(a-e) respectively. Graphs in 7(a-e) depict a consistent shift in heat conduction behaviour across various parameters. At low parameter values, the heat transfer rate initially rises and stabilizes over time. However, with an increase in any parameter, there's an initial jump followed by a gradual decline in heat transfer rate. Notably, increment in any of the parameters Le, Rn, λ, $\Pr$ or N_A results in the suppression of heat convection. An intriguing observation here is that this outcome stands in stark contrast to the convection in a Rivlin-Erickson nanofluid between parallel boundaries, as reported in reference [46].

Jilin Daxue Xuebao (Gongxueban)/Journal of Jilin University (Engineering and Technology Edition)
ISSN: 1671-5497
E-Publication: Online Open Access
Vol: 42 Issue: 11-2023
DOI: 10.5281/zenodo.10153201

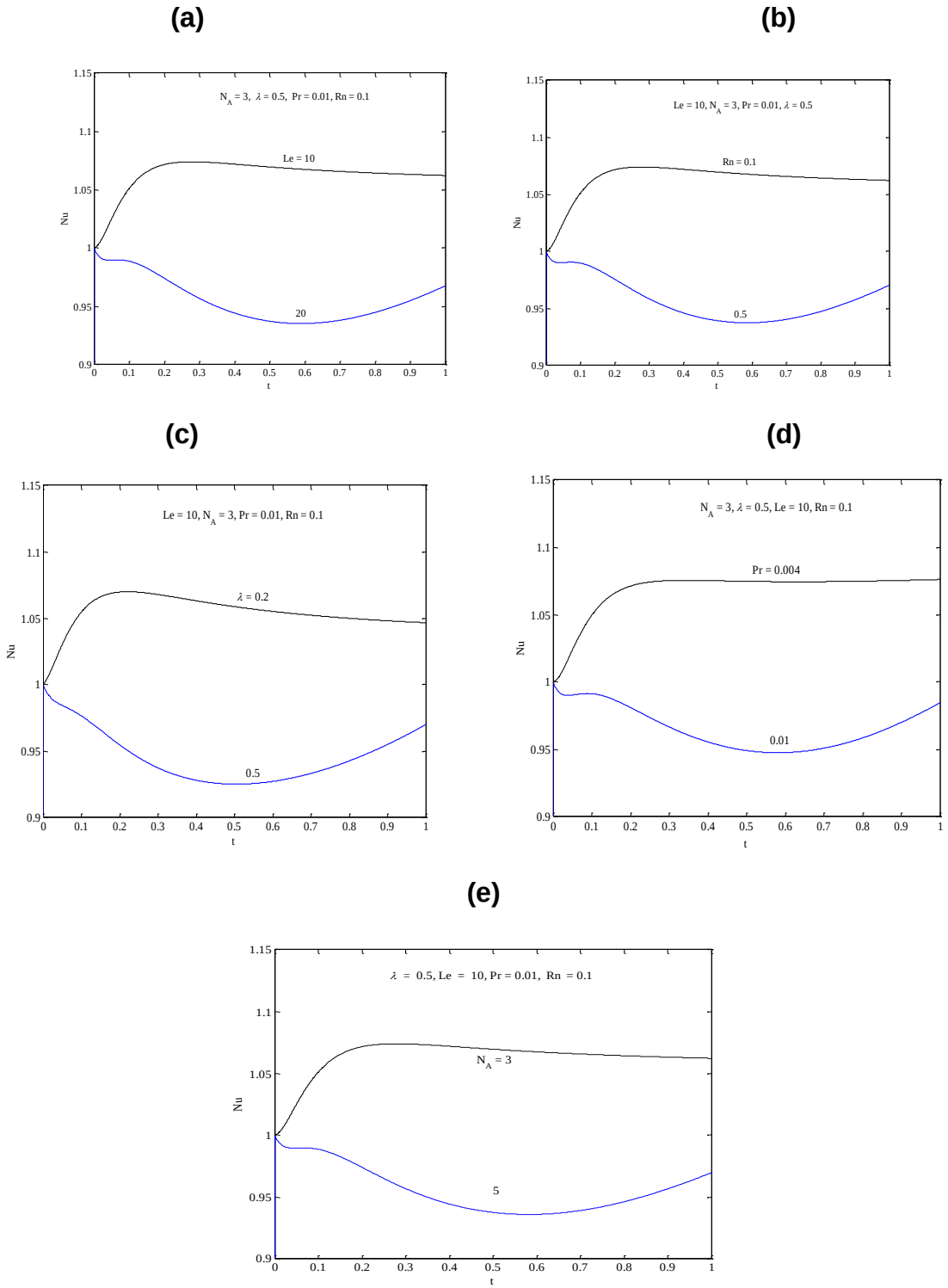

Fig.7: Variation in Nu with time for different values of (a) Le (b) Rn (c) λ (d) Pr

Jilin Daxue Xuebao (Gongxueban)/Journal of Jilin University (Engineering and Technology Edition)
ISSN: 1671-5497
E-Publication: Online Open Access
Vol: 42 Issue: 11-2023
DOI: 10.5281/zenodo.10153201

and (e) N_A

In Figs. 8(a-e) it is observed that initially the rate of transfer of mass increases but gradually decreases over time eventually showing a steady behaviour. It is observed that if any of the parameters N_A, λ, Rn and $\Pr$ is increased, Nu_ϕ decreases [Figs. 8(a-d)]. Again the behaviour of these parameters runs contrary to what was discussed in [29] and [46]. Regarding the Lewis number Le, it is unveiled that on its increment, the rate of transfer of mass is increased up to a certain time but as the time passes, it gradually decreases, reducing the mass transfer rate. (Fig. 8e). Thus, the Lewis number exhibits a dual behaviour resembling an exponential type, transitioning from initial vigorous oscillations to a steady rate, as seen in reference [31]. It is to be mentioned that in a Rivlin Erickson fluid [46], it just enhanced the mass transfer rate.

(a)

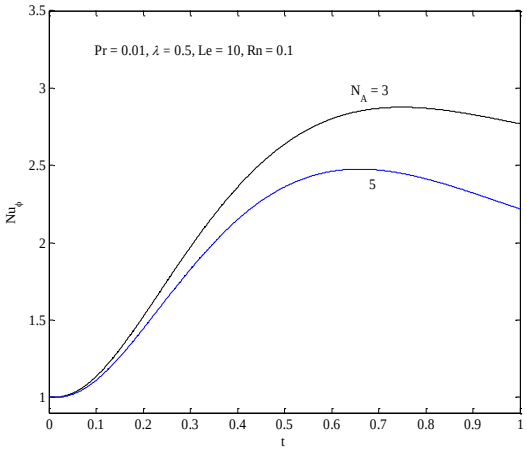

(b)

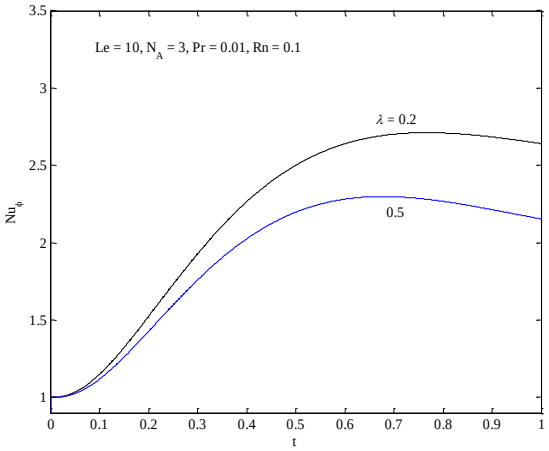

(c)

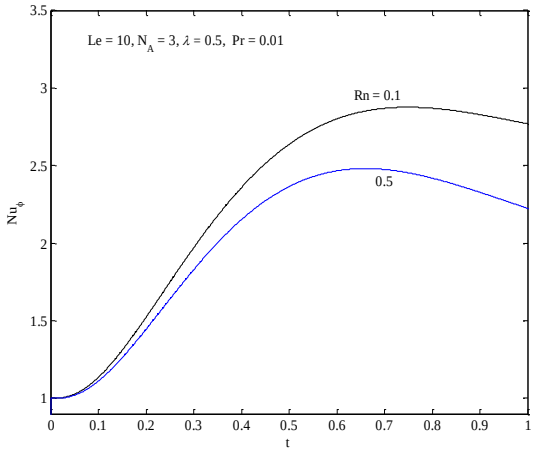

(d)

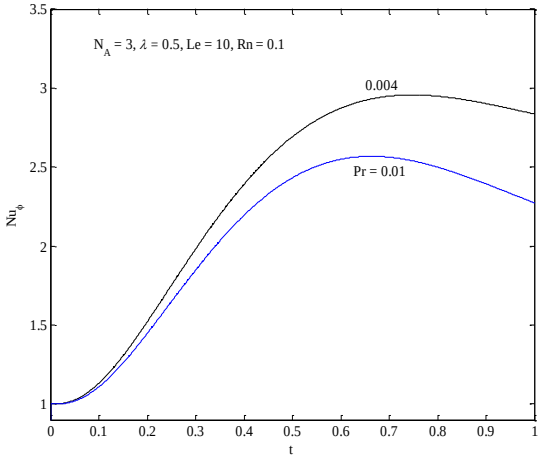

Jilin Daxue Xuebao (Gongxueban)/Journal of Jilin University (Engineering and Technology Edition)
ISSN: 1671-5497
E-Publication: Online Open Access
Vol: 42 Issue: 11-2023
DOI: 10.5281/zenodo.10153201

(e)

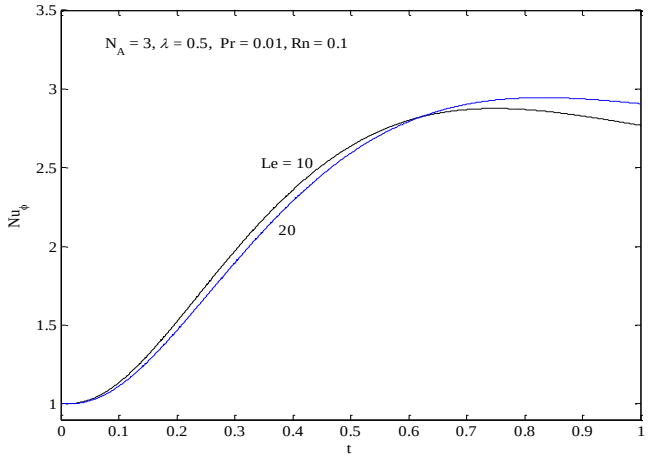

Fig.8: Variations in the concentration Nusselt number with time for different values of (a) N_A, (b) λ (c) Rn (d) $\Pr$ and (e) Le

In Fig. 9, we draw time-dependent streamlines, isotherms and isonanoconcentrations for $Ra^{cr} = 27\pi^4/4$, $Le = 10$, $Rn = 0.1$, $\lambda = 0.5$, $\Pr = 0.01$ and $N_A = 3$. Clearly, the magnitude of the stream function remains constant as time passes (Figs. 9a, 9b). As anticipated by Figures 9(c-d) for isotherms and 9(e-f) for isonanoconcentrations, the convective patterns grow more pronounced over time.

***t* = 0.006** ***t* = 0.01**

(a) **(b)**

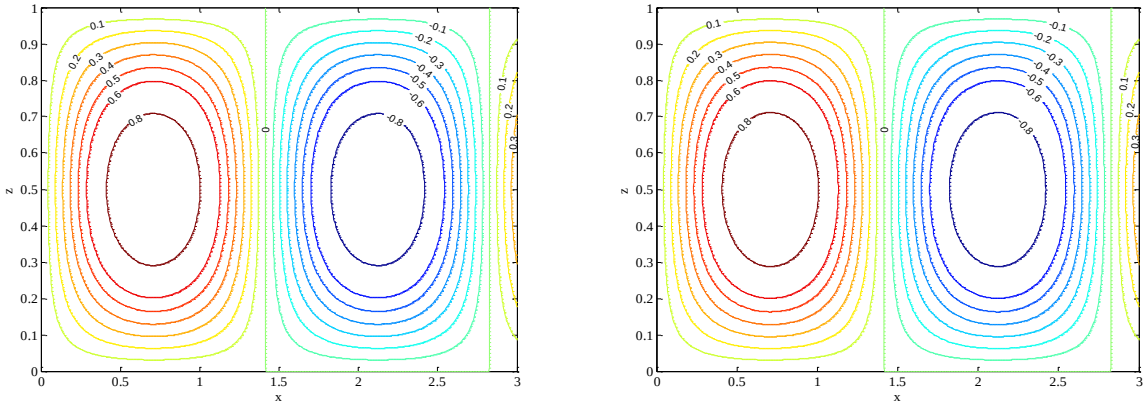

(c) **(d)**

Jilin Daxue Xuebao (Gongxueban)/Journal of Jilin University (Engineering and Technology Edition)
ISSN: 1671-5497
E-Publication: Online Open Access
Vol: 42 Issue: 11-2023
DOI: 10.5281/zenodo.10153201

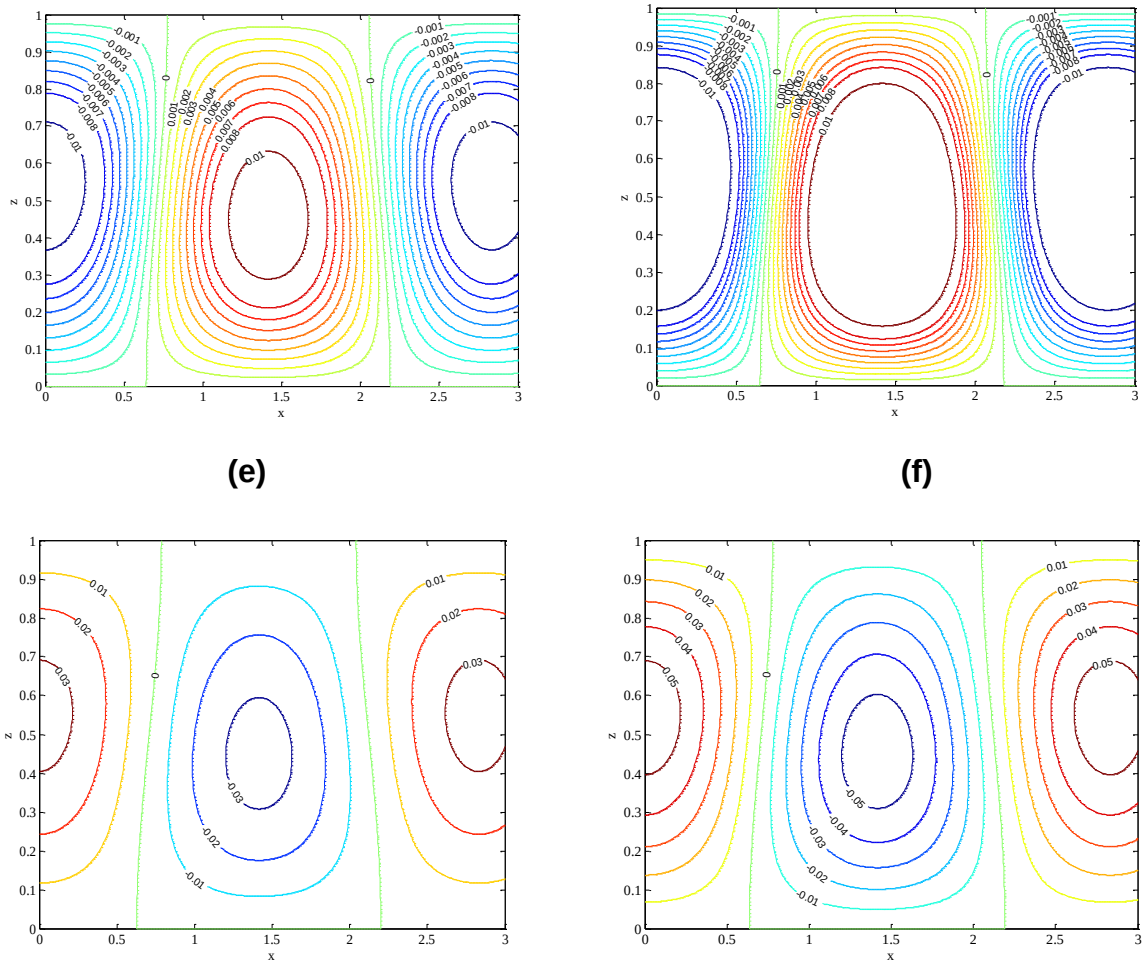

Fig.9: Variations of streamlines, isotherms and isonanoconcentrations with time

9. CONCLUSIONS

In this study, we have examined convection within a layer of Maxwell nanofluid constrained between two parallel plates, with no nanoparticle flux at the boundaries. Under the linear and non-linear stability theories following conclusions have been drawn:

9.1. Stationary and Oscillatory Convection

1. Nanoparticles trigger stationary convection at an earlier stage.
2. The Lewis number Le, concentration Rayleigh number Rn, and modified diffusivity ratio N_A destabilize the stationary convection.
3. Both the Lewis number Le and the Prandtl number Pr stabilize the oscillatory convection.

Jilin Daxue Xuebao (Gongxueban)/Journal of Jilin University (Engineering and Technology Edition)
ISSN: 1671-5497
E-Publication: Online Open Access
Vol: 42 Issue: 11-2023
DOI: 10.5281/zenodo.10153201

4. The concentration Rayleigh number Rn, the modified diffusivity ratio N_A, and the stress relaxation parameter λ destabilize the oscillatory convection.
5. Convection sets earlier in stationary mode of convection than transit to the oscillatory convection.

9.2. Steady State Convection

1. On increasing the modified diffusivity ratio N_A, and the concentration Rayleigh number Rn, enhancement in the rate of heat transfer is noticed while the Lewis number Le has a reverse effect.
2. In case of transfer of mass N_A, Rn, Le have dual behaviour.
3. The effect of N_A and Rn regarding the heat and mass transfer is in contrast to the effect of these parameters on a Maxwell nanofluid saturated in a porous medium.
4. The magnitude of stream function increases on increasing the Rayleigh number.
5. The mode of heat transfer initially appears in the form of convection for a small value of Rayleigh number, but as the Rayleigh number increases the convection falls weak and conduction becomes more prominent.
6. Mass transfer involves a combination of partial convection for low Rayleigh numbers, but for high Rayleigh numbers, mass transfer relies solely on diffusion.

9.2.2. Unsteady State Convection

1. In contrast to the convection in a Rivlin-Erickson fluid, there is a decline in the heat transfer rate.
2. Mass transfer rate decreases as time passes for increasing values of parameters N_A, λ, Rn and Pr but the Lewis number Le shows a dual character.
3. The behaviour of parameters N_A, λ, Rn and Pr is to depress the rate of transfer of mass which was supportive for a Maxwell fluid in a modified or a conventional Darcy Maxwell nanofluid.
4. The magnitude of the stream function remains constant as time passes.
5. Over time, both heat and mass transfer intensify through increasingly stronger convection.

Nomenclature

c	specific heat of fluid at constant pressure (J kg^{-1} K^{-1})
d	dimensional depth between two boundaries (m)
D_T	thermophoretic diffusion coefficient (m^2 s^{-1})
D_B	Brownian diffusion coefficient (m^2 s^{-1})

Jilin Daxue Xuebao (Gongxueban)/Journal of Jilin University (Engineering and Technology Edition)
ISSN: 1671-5497
E-Publication: Online Open Access
Vol: 42 Issue: 11-2023
DOI: 10.5281/zenodo.10153201

g acceleration due to gravity (m s^{-2})

k thermal conductivity of the nanofluid ($Wm^{-1}K^{-1}$)

Le nanofluid Lewis number

N_A modified diffusivity ratio

N_B modified particle density ratio

p^* hydrostatic pressure (Pa)

p dimensionless hydrostatic pressure

Pr nanofluid Prandtl number

Ra thermal Rayleigh number

Rn nanoparticle concentration Rayleigh number

T^* temperature (K)

T dimensionless temperature

T_c^* reference temperature at the upper boundary (K)

T_h^* temperature at the lower boundary (K)

t^* time (s)

t dimensionless time

$\mathbf{v}^*$ nanofluid velocity (s^{-1})

$\mathbf{v}$ dimensionless velocity

(u^*, v^*, w^*) velocity components

(x, y, z) dimensionless Cartesian coordinates

$(\rho c)_f$ heat capacity of nanofluid (J K^{-1})

$(\rho c)_p$ heat capacity of nanoparticles (J K^{-1})

Greek Symbols

ρ density of the base fluid (kg m^{-3})

ρ_p density of nanoparticles (kg m^{-3})

ω dimensionless frequency of oscillations

α dimensionless wave number

ψ dimensionless stream function

λ dimensionless stress relaxation time parameter

Jilin Daxue Xuebao (Gongxueban)/Journal of Jilin University (Engineering and Technology Edition)
ISSN: 1671-5497
E-Publication: Online Open Access
Vol: 42 Issue: 11-2023
DOI: 10.5281/zenodo.10153201

ϕ dimensionless volume fraction of nanoparticles

ϕ_0^* reference value of nanoparticle volume fraction

α_f thermal diffusivity ($m^2\ s^{-1}$)

β thermal expansion coefficient (K^{-1})

μ viscosity (Pa s)

Subscripts

b basic state value

c upper boundary

f fluid

h lower boundary

0 reference value

p nanoparticle

Superscripts

$*$ dimensional variable

$'$ infinitesimal perturbed variable

osc oscillatory convection mode

st stationary convection mode

Operators

$\nabla_H^2 \quad \frac{\partial^2}{\partial x^2}+\frac{\partial^2}{\partial y^2}$

$\nabla_1^2 \quad \frac{\partial^2}{\partial x^2}+\frac{\partial^2}{\partial z^2}$

$\nabla^2 \quad \nabla_H^2+\frac{\partial^2}{\partial z^2}$

Conflict of Interest Statement: The authors have no conflicts of interest.

References

1) Choi, S.U.S. and Eastman, J.A. (1995). Enhancing thermal conductivity of fluids with nanoparticles. ASME FED 66, 99–105.

2) Eastman, J. A., Choi, U. S., Li, S., Thompson, L. J. and Lee, S. (1996). Enhanced Thermal conductivity through the development of nanofluids. *MRS Online Proceedings Library*, 457, 3–11. https://doi.org/10.1557/PROC-457-3

3) Eastman, J. A., Choi, U. S., Li, S., Thompson, L. J. and Lee, S. (1997). Enhanced thermal conductivity through the development of nanofluids. In nanophase and nanocomposite materials II. Edited by: Komarneni S, Parker JC, Wollenberger HJ. *Pittsburg: Materials Research Society*, 3–11.

ISSN: 1671-5497
E-Publication: Online Open Access
Vol: 42 Issue: 11-2023
DOI: 10.5281/zenodo.10153201

4) Lee, S., Choi, S. U. S., Li, S. and Eastman, J. A. (1999). Measuring thermal conductivity of fluids containing oxide nanoparticles. *J. Heat Transfer*, 121(2), 280-289. https://doi.org/10.1115/1.2825978

5) Eastman, J. A., Choi, S. U. S., Li, S., Yu, W. and Thompson, L. J. (2001). Anomalously increased effective thermal conductivities of ethylene glycol-based nanofluids containing copper nanoparticles. *Appl. Phys. Lett.*, 78(6), 718–720. https://doi.org/10.1063/1.1341218

6) Hong, T. K., Yang, H. S. and Choi, C. J. (2005). Study of the enhanced thermal conductivity of Fe nanofluids. *J. Appl. Phys.*, 97(6), 064311. https://doi.org/10.1063/1.1861145

7) Yu, W., France, D. M., Routbort, J. L. and Choi, S.U.S. (2008). Review and comparison of nanofluid thermal conductivity and heat transfer enhancements. *Heat Transfer Engineering*, 29(5), 432–460. https://doi.org/10.1080/01457630701850851

8) Penkavova, V., Tihon, J. and Wein, O. (2011). Stability and rheology of dilute TiO_2-water nanofluids. *Nanoscale Res. Lett.*, 6, 273. https://doi.org/10.1186/1556-276X-6-273

9) Namburu, P.K., Kulkarni, D.P., Misra, D. and Das, D.K. (2007). Viscosity of copper oxide nanoparticles dispersed in ethylene glycol and water mixture. *Exp. Therm. Fluid Sci.*, 32(2), 397-402. https://doi.org/10.1016/j.expthermflusci.2007.05.001

10) Duan, F., Kwek, D. and Crivoi, A. (2011). Viscosity affected by nanoparticle aggregation in Al_2O_3-water nanofluids. *Nanoscale Res. Lett.*, 6, 248. https://doi.org/10.1186/1556-276X-6-248

11) Kulkarni, D.P., Das, D.K. and Chukwu, G.A. (2006). Temperature-dependent rheological property of copper oxide nanoparticles suspension (nanofluid). *Journal of Nanoscience and Nanotechnology*, 6(4), 1150-1154. https://doi.org/10.1166/jnn.2006.187

12) Buongiorno, J. et al. (2009). A benchmark study on the thermal conductivity of nanofluids. *J. Appl. Phys.*, 106(9), 094312. https://doi.org/10.1063/1.3245330

13) Venerus, D.C. et al. (2010). Viscosity measurements on colloidal dispersions (nanofluids) for heat transfer applications. *Appl. Rheol*., 20(4), 44582. https://doi.org/10.3933/applrheol-20-44582

14) *Chen, H., Ding, Y. and Tan, C. (2007). Rheological behaviour of nanofluids. New J. Phys., 9(10), 367.* https://doi.org/10.1088/1367-2630/9/10/367

15) *Chen, H. and Ding, Y. (2009). Heat transfer and rheological behaviour of nanofluids – a review. In: Wang, L. (eds) Advances in Transport Phenomena, 1, 135-177.* https://doi.org/10.1007/978-3-642-02690-4_3

16) Hojjat, M., Etemad, S. Gh, Bagheri, R. and Thibault, J. (2011). Rheological characteristics of non-Newtonian nanofluids: experimental investigation. *Int. Commun. Heat Mass Transfer*, 38(2), 144–148. https://doi.org/10.1016/j.icheatmasstransfer.2010.11.019

17) Sharma, A. K., Tiwari, A. K. and Dixit, A. R. (2016). Rheological behaviour of nanofluids: a review. *Renew. Sust. Energ. Rev*., 53, 779-791, https://doi.org/10.1016/j.rser.2015.09.033

18) Murshed, S. M. S. and Estellé, P. (2017). A state of the art review on viscosity of nanofluids. *Renew. Sust. Energ. Rev*., 76, 1134-1152. https://doi.org/10.1016/j.rser.2017.03.113

19) Minakov, A. V., Rudyak, V. Y. and Pryazhnikov, M. I. (2018). About rheology of nanofluids. *AIP Conf. Proc*., 2027(1), 030141. https://doi.org/10.1063/1.5065235

20) **Yapici, K., Osturk, O.** and **Uludag, Y.** (2018). Dependency of nanofluid rheology on particle size and concentration of various metal oxide nanoparticles. *Braz. J. Chem. Eng.*, 35 (2), 575-586. https://doi.org/10.1590/0104-6632.20180352s20160172

21) Khan, I., Bhat, A.H., Sharma, D.K., Usmani, M. and Khan, F. (2019). Overview of nanofluids to ionanofluids: applications and challenges. In: Bhat A., Khan I., Jawaid M., Suliman F., Al-Lawati H., Al-Kindy S. (eds) *Nanomaterials for Healthcare, Energy and Environment*. *Advanced Structured Materials*, 118. Springer, Singapore. https://doi.org/10.1007/978-981-13-9833-9_10

ISSN: 1671-5497
E-Publication: Online Open Access
Vol: 42 Issue: 11-2023
DOI: 10.5281/zenodo.10153201

22) Le Ba, T., Alkurdi, A. Q., Lukács, I. E., Molnár, J., Wongwises, S., Gróf, G. and Szilágyi, I. M. (2020). A novel experimental study on the rheological properties and thermal conductivity of Halloysite nanofluids. *Nanomaterials*, 10(9), 1834. http://dx.doi.org/10.3390/nano10091834

23) Sharma, A.K., Singh, R.K., Tiwari, A.K., Dixit, A.R. and Katiyar, J.K. (2020). Rheological behaviour of hybrid nanofluids: a review. In: Katiyar, J., Ramkumar, P., Rao, T., Davim, J. (eds) *Tribology in Materials and Applications. Materials Forming, Machining and Tribology*. Springer, Cham., 77-94. https://doi.org/10.1007/978-3-030-47451-5_4

24) Ali, N. *et al.* (2021). Carbon-based nanofluids and their advances towards heat transfer applications- a review. *Nanomaterials (Basel, Switzerland)*, *11*(6), 1628. https://doi.org/10.3390/nano11061628

25) Anju, P., Aryanandiny, B., Amizhtan, S. K., Gardas, R. L. and Sarathi, R. (2022). Investigation on the electrical and rheological properties of AlN-based synthetic ester nanofluids. in IEEE *Access*, 10, 37495-37505. DOI: 10.1109/ACCESS.2022.3163374.

26) Harchaoui, A., Mazouzi, R. and Karas, A. (2023). The Rheology of nanolubricants based on Fe_2O_3, Al_2O_3, and ZnO oxide nanoparticles: a comparative study. *Physical Chemistry Research*, *11*(2), 181-189. DOI: 10.22036/pcr.2022.328709.2027

27) Maxwell, J. C. (1867). On the dynamical theory of gases. *Phil. Trans. R. Soc. Lond*., 157, 49-88. https://doi.org/10.1098/rstl.1867.0004

28) Umavathi, J.C., Yadav, D. and Mohite, M. B. (2015). Linear and nonlinear stability analyses of double-diffusive convection in a porous medium layer saturated in a Maxwell nanofluid with variable viscosity and conductivity. *Elixir Mech. Engg.*, 79, 30407-30426.

29) Umavathi, J.C. and Mohite, M. B. (2016). Convective transport in a porous medium layer saturated with a Maxwell nanofluid. *Journal of King Saud University - Engineering Science,* 28(1), 56–68. https://doi.org/10.1016/j.jksues.2014.01.002

30) Ramzan, M., Bilal, M., Chung, J. D. and Farooq, U. (2016). Mixed convective flow of Maxwell nanofluid past a porous vertical stretched surface – an optimal solution. *Results in Physics*, 6, 1072-1079. https://doi.org/10.1016/j.rinp.2016.11.036

31) Jaimala, Singh, J. and Tyagi, V. K. (2017). A macroscopic filtration model for natural convection in a Darcy Maxwell nanofluid saturated porous layer with no nanoparticle flux at the boundary. *Int. J. Heat Mass Transf*., 111, 451-466. https://doi.org/10.1016/j.ijheatmasstransfer.2017.04.003

32) Jaimala, Singh, J. and Tyagi, V. K. (2018). Stability of double-diffusive convection in a Darcy porous layer saturated with Maxwell nanofluid under macroscopic filtration law: a realistic approach. *Int. J. Heat Mass Transf.*, 125, 290–309. https://doi.org/10.1016/j.ijheatmasstransfer.2018.04.070

33) Sharma, V., Chowdhary, A. and Gupta, U. (2018). Electrothermal convection in dielectric Maxwellian nanofluid layer. *Journal of Applied Fluid Mechanics*, *11*(3), 765-777. DOI: 10.29252/jafm.11.03.27905

34) Singh, R., Bishnoi, J. and Tyagi, V.K., (2019). The onset of Soret-driven instability in a Darcy–Maxwell nanofluid. *SN Appl. Sci.*, 1, 1273. https://doi.org/10.1007/s42452-019-1325-3

35) Singh, R., Bishnoi, J. and Tyagi, V.K. (2020). Triple diffusive convection with Soret–Dufour effects in a Maxwell nanofluid saturated in a Darcy porous medium. *SN Appl. Sci.*, 2, 704. https://doi.org/10.1007/s42452-020-2462-4

36) Aziz, A. and Shams, M. (2020). Entropy generation in MHD Maxwell nanofluid flow with variable thermal conductivity, thermal radiation, slip conditions, and heat source. *AIP Advances,* 10 (1), 015038. https://doi.org/10.1063/1.5129569

37) Xu, Y. J., Bilal, M., Al-Mdallal, Q., Khan, M.A. and Muhammad, T. (2021). Gyrotactic micro-organism flow of Maxwell nanofluid between two parallel plates. *Sci Rep*, 11(1), 15142. https://doi.org/10.1038/s41598-021-94543-4

ISSN: 1671-5497
E-Publication: Online Open Access
Vol: 42 Issue: 11-2023
DOI: 10.5281/zenodo.10153201

38) Khan, N., Ali, F., Arif, M., Ahmad, Z., Aamina, A. and Khan, I. (2021). Maxwell nanofluid flow over an infinite vertical plate with ramped and isothermal wall temperature and concentration. *Mathematical Problems in Engineering*, 2021, 3536773. https://doi.org/10.1155/2021/3536773

39) Wang, F., Ahmad, S., Al Mdallal, Q. et al. (2022). Natural bio-convective flow of Maxwell nanofluid over an exponentially stretching surface with slip effect and convective boundary condition. *Sci Rep*, 12, 2220. https://doi.org/10.1038/s41598-022-04948-y

40) Khan, N., Ali, F., Ahmad, Z. et al. (2023). A time fractional model of a Maxwell nanofluid through a channel flow with applications in grease. *Sci Rep*, 13, 4428. https://doi.org/10.1038/s41598-023-31567-y

41) E. Sangeetha, P. De and R. Das (2023). Hall and ion effects on bioconvective Maxwell nanofluid in non-Darcy porous medium, *Spec. Top. Rev. Porous Media: Int. J.*, 14(4), 1-30, DOI: 10.1615/SpecialTopicsRevPorousMedia.v14.i4.10

42) D.A. Nield, and A.V. Kuznetsov (2009). Thermal instability in a porous medium layer saturated by a nanofluid, *Int. J. Heat Mass Transf.*, 52 (25–26), 5796-5801. https://doi.org/10.1016/j.ijheatmasstransfer.2009.07.023

43) Baehr, H. D. and Stephan, K. (2011). Heat and Mass Transfer. 3rd edition, Springer Berlin, Heidelberg. https://doi.org/10.1007/978-3-642-20021-2

44) Nield, D.A. and Kuznetsov, A.V. (2014). Thermal instability in a porous medium layer saturated by a nanofluid: a revised model. *Int. J. Heat Mass Transf*., 68, 211–214. https://doi.org/10.1016/j.ijheatmasstransfer.2013.09.026

45) Buongiorno, J. (2006). Convective transport in nanofluids. *ASME J. Heat Transfer*, 128(3), 240-250. https://doi.org/10.1115/1.2150834

46) Bishnoi, J., Kumar, S. and Tyagi, R. (2023). Thermal convection of Rivlin-Ericksen fluid governed by the Brownian motion and thermophoresis of nanoparticles with passive behaviour of nanoparticles at the Parallel Boundaries. *J. Nanofluids*, 12(5), 1194–1209. DOI:10.1166/jon.2023.2010

47) Jaimala and Goyal, N. (2012). Soret Dufour driven thermosolutal instability of Darcy-Maxwell fluid. *IJE Transactions A: Basics*, 25(4), 367-378. https://www.ije.ir/article_72060.html

48) Bhadauria, B.S. and Agarwal, S. (2011). Natural convection in a nanofluid saturated rotating porous layer: a nonlinear study. *Transp Porous Media*, 87, 585–602. https://doi.org/10.1007/s11242-010-9702-9

49) Agarwal, S. (2014). Natural convection in a nanofluid-saturated rotating porous layer: a more realistic approach. *Transp Porous Media*, 104(3),581–592. https://doi.org/10.1007/s11242-014-0351-2

50) Agarwal, S., Rana, P. and Bhadauria, B.S. (2014). Rayleigh-Bénard convection in a nanofluid layer using a thermal nonequilibrium model. *J. Heat Transfer*, 136(12), 122501. https://doi.org/10.1115/1.4028491

51) Chand, R. and Rana, G.C. (2014). Thermal instability in a Brinkman porous medium saturated by nanofluid with no nanoparticle flux on boundaries. *Spec. Top. Rev. Porous Media: Int. J.*, 5(4), 277–286. DOI: 10.1615/SpecialTopicsRevPorousMedia.v5.i4.10

52) Shivkumara, I.S. and Dhananjaya, M. (2014). Onset of convection in a nanofluid saturated porous layer with temperature dependent viscosity. *Int. J. Eng. Res. Appl*., 4(4), 80–85.

53) Rana, G.C., Thakur, R.C. and Kango, S.K. (2014). On the onset of thermosolutal instability in a layer of an elastico-viscous nanofluid in porous medium. *FME Trans*., 42(1), 1–9. https://doi.org/10.5937/fmet1401001R

Jilin Daxue Xuebao (Gongxueban)/Journal of Jilin University (Engineering and Technology Edition)
ISSN: 1671-5497
E-Publication: Online Open Access
Vol: 42 Issue: 11-2023
DOI: 10.5281/zenodo.10153201

54) Shivkumara, I.S. and Dhananjaya, M. (2015). Penetrative Brinkman convection in an anisotropic porous layer saturated by a nanofluid. *AIN Shams Eng. J*., 6(2), 703–713. https://doi.org/10.1016/j.asej.2014.12.005

55) Yadav, D. and Lee, J. (2016). Onset of convection in a nanofluid layer confined within a Hele-Shaw cell. *J. Appl. Fluid Mech*., 9 (2), 519–527. https://doi.org/10.18869/acadpub.jafm.68.225.24433

56) Yadav, D., Lee, D., Cho, H.H. and Lee, J. (2016). The onset of double-diffusive nanofluid convection in a rotating porous medium layer with thermal conductivity and viscosity variation: a revised model. *J. Porous Media*, 19 (1), 31–46. DOI: 10.1615/JPorMedia.v19.i1.30

57) Chand, R., Rana, G.C. and Yadav, D. (2016). Electrothermo convection in a porous medium saturated by nanofluid. *J. Appl. Fluid Mech*., 9 (3), 1081–1088. https://doi.org/10.18869/acadpub.jafm.68.228.24858

58) Yadav, D., Agrawal, G.S. and Lee, J. (2016). Thermal instability in a rotating nanofluid layer: a revised model. *AIN Shams Eng. J*., 7 (1), 431–440. https://doi.org/10.1016/j.asej.2015.05.005

59) Rana, G.C. and Chand, R. (2015). Stability analysis of double-diffusive convection of RivlinEricksen elastico-viscous nanofluid saturating a porous medium: a revised model. *Forsch. Ingenieurwes*., 79 (1-2), 87–95. https://doi.org/10.1007/s10010-015-0190-5

60) Sharma, J., Gupta, U., Wanchoo, R.K. and Ahuja, J. (2016). An analytical and numerical study for thermosolutal nanofluid convection using revised model. *Recent Trends Eng. Mater. Sci*. (*Perspectives in Science*), 8,495–497. https://doi.org/10.1016/j.pisc.2016.05.006